

$\Lambda\alpha$, $\Sigma\alpha$ and $\Xi\alpha$ potentials derived from the SU_6 quark-model baryon-baryon interaction

Y. Fujiwara, M. Kohno* and Y. Suzuki**

Department of Physics, Kyoto University, Kyoto 606-8502, Japan

**Physics Division, Kyushu Dental College, Kitakyushu 803-8580, Japan*

***Department of Physics, and Graduate School of Science and Technology,
Niigata University, Niigata 950-2181, Japan*

Abstract

We calculate $\Lambda\alpha$, $\Sigma\alpha$ and $\Xi\alpha$ potentials from the nuclear-matter G -matrices of the SU_6 quark-model baryon-baryon interaction. The α -cluster wave function is assumed to be a simple harmonic-oscillator shell-model wave function. A new method is proposed to derive the direct and knock-on terms of the interaction Born kernel from the hyperon-nucleon G -matrices, with explicit treatments of the nonlocality and the center-of-mass motion between the hyperon and α . We find that the SU_6 quark-model baryon-baryon interactions, FSS and fss2, yield a reasonable bound-state energy for ${}^5_\Lambda\text{He}$, $-3.18 \sim -3.62$ MeV, in spite of the fact that they give relatively large depths for the Λ single-particle potentials, $46 \sim 48$ MeV, in symmetric nuclear matter. An equivalent local potential derived from the Wigner transform of the nonlocal $\Lambda\alpha$ kernel shows a strong energy dependence for the incident Λ -particle, indicating the importance of the strangeness-exchange process in the original hyperon-nucleon interaction. For the $\Sigma\alpha$ and $\Xi\alpha$ potentials, we only discuss the zero-momentum Wigner transform of the interaction kernels, since these interactions turn out to be repulsive when the two isospin contributions for the ΣN and ΞN interactions are added up. These components show a strong isospin dependence: They are attractive in the isospin $I = 1/2$ ($\Sigma\alpha$) and $I = 0$ ($\Xi\alpha$) components and repulsive in $I = 3/2$ ($\Sigma\alpha$) and $I = 1$ ($\Xi\alpha$) components, which indicate that Σ and Ξ potentials could be attractive in some particular systems such as the well-known ${}^4_2\text{He}$ system.

Key words: $\Lambda\alpha$ potential, YN interaction, quark model baryon-baryon interaction, G -matrix, single-particle spin-orbit potential of hyperons

PACS: 13.75.Cs, 12.39.Jh, 13.75.Ev, 24.85.+p, 21.60.Gx, 21.80.+a

1 Introduction

Interactions between the octet baryons ($B_8 = N, \Lambda, \Sigma$ and Ξ) and the α cluster are important ingredients to consider the possible existence for various kinds of light hypernuclei through detailed microscopic cluster-model calculations. If reliable effective B_8N interactions were known, one could easily calculate the $B_8\alpha$ potentials, using the standard cluster-model techniques. Unfortunately, this is not the case except for $B_8 = N$, since the bare B_8N interaction itself is not well known especially for the Σ and Ξ hyperons, because of the technical difficulties of strangeness experiments. Even if these bare interactions were eventually known, we further need to develop the procedure to link the bare interactions and effective interactions through some effective interaction theory such as the G -matrix formalism.

We have recently developed the QCD-inspired spin-flavor SU_6 quark model for the baryon-baryon interaction [1], which is a unified model for the full octet-baryons [2], and have achieved accurate descriptions of the NN and YN interactions [3]. In particular, the NN interaction of the most recent model fss2 is accurate enough to compare with modern realistic meson-exchange models. These quark-model interactions were used for the detailed study of few-baryon systems such as ${}^3\text{H}$ [4,5] and ${}^3_\Lambda\text{H}$ [6], and also of some typical Λ -hypernuclei, ${}^9_\Lambda\text{Be}$ [7,8] and ${}^6_{\Lambda\Lambda}\text{He}$ [9], through a newly developed three-cluster Faddeev formalism [10,11] and G -matrix calculations [12,13,14]. We can now use these baryon-baryon interactions to calculate not only the $\Lambda\alpha$ interaction, but also $\Sigma\alpha$ and $\Xi\alpha$ interactions, assuming the harmonic-oscillator (h.o.) shell-model wave function for the α -cluster.

There are, in fact, a couple of advanced procedure to derive the interactions between a single baryon and finite nuclei based on the density-dependent Hartree-Fock theory of G -matrix interactions [15,16,17]. These approaches, however, use the localized G -matrix interaction in the configuration space and the center-of-mass (c.m.) coordinate system connected to the target nucleus. For the $B_8\alpha$ interactions, the c.m. correction is quite important. In this paper, we will derive $B_8\alpha$ Born kernels, directly starting from the G -matrix calculation of the quark-model baryon-baryon interactions. We deal with the nonlocality of the G -matrix and the c.m. motion exactly, using the cluster-model approach, at the expense of the self-consistency between the α -cluster formation and the G -matrix interaction. The G -matrix is pre-determined by solving the Bethe-Goldstone equation in symmetric nuclear matter, and the momentum-dependent single-particle (s.p.) potentials as well [12]. The Fermi-momentum is assumed to be the standard value $k_F = 1.35 \text{ fm}^{-1}$, but the obtained $B_8\alpha$ interactions depend on this choice very little, except for some special cases such as the $\Lambda\alpha$ LS interaction. The treatment of the starting-energy dependence and the non-Galilean invariant momentum dependence of

the G -matrix is explicitly discussed. We believe that these approximations are good enough to understand the unknown $\Sigma\alpha$ and $\Xi\alpha$ interactions qualitatively, starting from the quark-model predictions of various baryon-baryon interactions. For the $\Lambda\alpha$ interaction, we compare the predictions by the present approach with some available phenomenological $\Lambda\alpha$ potentials [7,18], obtained by various methods. Another application of the present approach to the $N\alpha$ interaction will be published in a separate paper, since this system involves an extra nucleon-exchange term.

Since the obtained $B_8\alpha$ interactions are all nonlocal, we calculate the Wigner transform from the $B_8\alpha$ Born kernels. We find that the momentum dependence of the Wigner transform is very strong, and the procedure to find effective local potential by solving the transcendental equation is necessary to obtain a local-potential image for the $\Lambda\alpha$ interaction. The $\Sigma\alpha$ and $\Xi\alpha$ interactions are repulsive, although the isospin $I = 1/2$ (for $\Sigma\alpha$) and $I = 0$ (for $\Xi\alpha$) contributions of the ΣN and ΞN interactions are attractive. As the first step to study realistic $\Sigma\alpha$ and $\Xi\alpha$ interactions, we will only discuss the zero-momentum Wigner transform in this paper. Although these $B_8\alpha$ interactions are complex due to the imaginary part of the underlying G -matrices, we discuss only the real part. The spin-orbit $B_8\alpha$ potentials are naturally obtained from the LS and $LS^{(-)}$ components of the G -matrix invariant amplitudes.

The organization of this paper is as follows. In the next formulation section, we first give in Section 2.1 the basic folding formula for the α -cluster based on the separation of the $B_8\alpha$ Born kernel to the spin-isospin factors and the spatial part. The treatment of G -matrix variables, the starting energy and the c.m. momentum, will be carefully discussed. A convenient transformation formula for the rearrangement of relative momenta is given in Section 2.2, by which the partial wave component of the $B_8\alpha$ Born kernel is explicitly given both for the central component and the LS component. The folding formula in the partial-wave expansion and the partial-wave components of the $B_8\alpha$ Born kernel are explicitly given in Section 2.3. A procedure to calculate the Wigner transform is given in Section 2.4 with a couple of approximations. One of the approximations for the LS component yields a simple factor for the strength of the LS potential, which corresponds to the well-known Scheerbaum factor S_B [19] in nuclear matter. The Section 3 is devoted to the result and discussion; first in Section 3.1 the $\Lambda\alpha$ central and LS potentials both in the T -matrix approach and in the Wigner transform approach. The isospin dependence of the $\Sigma\alpha$ and $\Xi\alpha$ potentials are discussed in Section 3.2. Section 4 is devoted to a summary. The invariant G -matrix for the most general B_8B_8 interaction is discussed in Appendix A.

2 Formulation

2.1 α -cluster folding for the G -matrix invariant amplitudes

The $B_8\alpha$ Born kernel for the (0s) h.o. α -cluster wave function is calculated from

$$V(\mathbf{q}_f, \mathbf{q}_i) = \langle \delta(\mathbf{X}_G) e^{i\mathbf{q}_f \cdot \mathbf{r}} \chi_B \phi_\alpha | \sum_{j=2}^5 G_{1j} | 1 \cdot e^{i\mathbf{q}_i \cdot \mathbf{r}} \chi_B \phi_\alpha \rangle , \quad (2.1)$$

where χ_B is the spin-isospin wave function of B , ϕ_α the internal wave function of α , and G_{1j} the BN G -matrix acting on the particle $i = 1$ (B) and $j = 2 - 5$ (nucleons). We use the short-hand notation B to specify one of the octet baryons, $B_8 = N, \Lambda, \Sigma$ or Ξ . In Eq. (2.1), it is important to calculate the Born kernel in the total c.m. system by inserting $\delta(\mathbf{X}_G)$ and 1 in the bra and ket sides, respectively [20], since the G -matrix interaction G_{1j} is non-Galilean invariant. Namely, the two-particle G -matrix which satisfies the translational invariance is parametrized by

$$\langle \mathbf{p}_1, \mathbf{p}_2 | G | \mathbf{p}'_1, \mathbf{p}'_2 \rangle = \delta(\mathbf{K} - \mathbf{K}') \frac{1}{(2\pi)^3} G(\mathbf{p}, \mathbf{p}'; K, \omega, k_F) . \quad (2.2)$$

Here, ω is the starting energy, $K = |\mathbf{K}|$ is the magnitude of the c.m. momentum, k_F is the Fermi momentum of nuclear matter, and the relative momentum \mathbf{p} (and also \mathbf{p}' etc. with primes), is given by

$$\begin{aligned} \mathbf{p} &= \frac{\xi \mathbf{p}_1 - \mathbf{p}_2}{1 + \xi} , & \mathbf{p}_1 &= \frac{1}{1 + \xi} \mathbf{K} + \mathbf{p} , \\ \mathbf{K} &= \mathbf{p}_1 + \mathbf{p}_2 , & \mathbf{p}_2 &= \frac{\xi}{1 + \xi} \mathbf{K} - \mathbf{p} , \end{aligned} \quad (2.3)$$

with $\xi = (M_N/M_B) \leq 1$ being the mass ratio between the nucleon and the baryon B .¹ We assume a constant $k_F = 1.35 \text{ fm}^{-1}$ in this paper unless otherwise specified, so that we will omit this index in the following. In fact, the G -matrix in Eq. (2.1) contains the exchange term. It is, therefore, convenient to use the isospin sum of the invariant G -matrix, $G_{BB}^I(\mathbf{p}, \mathbf{p}'; K, \omega)$ with $I = I_B + 1/2$ and $I_B - 1/2$ (I_B is the isospin of B), defined through

$$\begin{aligned} &G_{BB}^I(\mathbf{p}, \mathbf{p}'; K, \omega) \\ &= \langle [BN]_{II_z} | G(\mathbf{p}, \mathbf{p}'; K, \omega) - G(\mathbf{p}, -\mathbf{p}'; K, \omega) P_\sigma P_F | [BN]_{II_z} \rangle \\ &= (1 + \delta_{B,N}) \left[g_0^I + g_{ss}^I(\boldsymbol{\sigma}_1 \cdot \boldsymbol{\sigma}_2) + h_0^I i\hat{\mathbf{n}} \cdot (\boldsymbol{\sigma}_1 + \boldsymbol{\sigma}_2) + h_-^I i\hat{\mathbf{n}} \cdot (\boldsymbol{\sigma}_1 - \boldsymbol{\sigma}_2) \right. \\ &\quad \left. + \dots \right] \end{aligned} \quad (2.4)$$

¹ Note that ζ used in Appendix B of Ref. [7] is the inverse of ξ .

Here $\hat{\mathbf{n}} = [\mathbf{p}' \times \mathbf{p}] / (p' p \sin \theta)$, and the invariant functions g_0^I (central), g_{ss}^I (spin-spin), h_0^I (LS), h_-^I ($LS^{(-)}$), etc. are functions of \mathbf{p}^2 , \mathbf{p}'^2 , $\cos \theta = (\hat{\mathbf{p}} \cdot \hat{\mathbf{p}}')$, K , ω , and k_F . These are expressed by the partial-wave components of the BN G -matrix as (see Appendix D of Ref. [21])

$$\begin{aligned}
\left. \begin{array}{l} g_0^I \\ g_{ss}^I \end{array} \right\} &= \frac{1}{4} \sum_{J \ell S} (2J+1) \left\{ \begin{array}{c} 1 \\ \frac{1}{3}[2S(S+1)-3] \end{array} \right\} G_{S\ell, S\ell}^{IJ} P_\ell(\cos \theta) \quad , \\
h_0^I &= -\frac{1}{4} \sum_J \frac{(2J+1)}{J(J+1)} \left[G_{1J, 1J}^{IJ} P_J^1(\cos \theta) \right. \\
&\quad \left. + J G_{1J+1, 1J+1}^{IJ} P_{J+1}^1(\cos \theta) - (J+1) G_{1J-1, 1J-1}^{IJ} P_{J-1}^1(\cos \theta) \right] \quad , \\
h_-^I &= \frac{1}{4} \sum_J \frac{(2J+1)}{\sqrt{J(J+1)}} \left[G_{1J, 0J}^{IJ} + G_{0J, 1J}^{IJ} \right] P_J^1(\cos \theta) \quad , \quad (2.5)
\end{aligned}$$

where the argument \mathbf{p} , \mathbf{p}' , K , ω , k_F and subscripts for the baryon channels are omitted for the typographical reason. In the LS term, $P_J^1(\cos \theta) = (\sin \theta) P_J'(\cos \theta)$ with $J \geq 1$ is the associated Legendre function of the first rank. The invariant G -matrix for the most general $B_8 B_8$ interaction is discussed in Appendix A.

In order to calculate the spin-isospin factors, it is convenient to introduce an isospin *pseudo*-exchange operator of the BN system by

$$P_\tau = \frac{1}{2I_B + 1} (1 + \tau_B \cdot \tau_N) \quad , \quad (2.6)$$

with the isospin matrix elements

$$(\tau_B \cdot \tau_N) = \begin{cases} 2I_B \\ -2(I_B + 1) \end{cases} \quad \text{for} \quad I = \begin{cases} I_B + 1/2 \\ I_B - 1/2 \end{cases} \quad , \quad (2.7)$$

and write the invariant G -matrix as

$$G(\mathbf{p}, \mathbf{p}'; K, \omega) = G_{BB}^{I=I_B+1/2}(\mathbf{p}, \mathbf{p}'; K, \omega) \frac{1+P_\tau}{2} + G_{BB}^{I=I_B-1/2}(\mathbf{p}, \mathbf{p}'; K, \omega) \frac{1-P_\tau}{2} \quad . \quad (2.8)$$

We need to calculate

$$X_B^{I\Omega} = \langle \chi_{B\alpha} | \sum_{j=2}^5 \omega_{1,j}^\Omega \left(\frac{1 \pm P_\tau}{2} \right)_{1,j} | \chi_{B\alpha} \rangle \quad , \quad (2.9)$$

with the spin factors $\omega_{12}^{central} = 1$, $\omega_{12}^{ss} = (\boldsymbol{\sigma}_1 \cdot \boldsymbol{\sigma}_2)$, $\omega_{12}^{LS} = \boldsymbol{\sigma}_1 + \boldsymbol{\sigma}_2$, and $\omega_{12}^{LS^{(-)}} = \boldsymbol{\sigma}_1 - \boldsymbol{\sigma}_2$. In Eq. (2.9), χ_α is the spin-isospin wave function of α ; i.e.,

$\phi_\alpha = \chi_\alpha \phi_\alpha^{\text{space}}$. Then we find that non-zero matrix elements are

$$X_B^{I \text{ central}} = 2 \frac{2I+1}{2I_B+1} \quad , \quad X_B^{I LS} = X_B^{I LS^{(-)}} = 2 \frac{2I+1}{2I_B+1} \boldsymbol{\sigma}_1 \quad . \quad (2.10)$$

On the other hand, the spatial part is calculated in Appendix (B6) of Ref. [7]. It is convenient to express this formula as

$$\begin{aligned} V^{\text{space}}(\mathbf{q}_f, \mathbf{q}_i) &= \langle \delta(\mathbf{X}_G) e^{i\mathbf{q}_f \cdot \mathbf{r}} \phi_\alpha^{\text{space}} | G^{\text{space}} | 1 \cdot e^{i\mathbf{q}_i \cdot \mathbf{r}} \phi_\alpha^{\text{space}} \rangle \\ &= e^{-\frac{3}{32\nu} k^2} \left(\frac{2(1+\xi)^2}{3\pi\nu} \right)^{\frac{3}{2}} \int d\mathbf{p} \exp \left\{ -\frac{2(1+\xi)^2}{3\nu} \left(\mathbf{p} - \frac{1+4\xi}{4(1+\xi)} \mathbf{q} \right)^2 \right\} \\ &\quad \times G^{\text{space}} \left(\mathbf{p} + \frac{1}{2} \mathbf{k}, \mathbf{p} - \frac{1}{2} \mathbf{k}; (1+\xi) |\mathbf{q} - \mathbf{p}|, \omega \right) \quad , \end{aligned} \quad (2.11)$$

where

$$\mathbf{k} = \mathbf{q}_f - \mathbf{q}_i \quad , \quad \mathbf{q} = \frac{1}{2} (\mathbf{q}_f + \mathbf{q}_i) \quad , \quad (2.12)$$

are the momentum transfer and the local momentum of the $B_8\alpha$ system. By assuming g_0^I , $h_0^I i\hat{\mathbf{n}}$ and $h_-^I i\hat{\mathbf{n}}$ for G^{space} , we finally obtain

$$\begin{aligned} V(\mathbf{q}_f, \mathbf{q}_i) &= \sum_{I\Omega} 2 \left(\frac{2I+1}{2I_B+1} \right) V^{I\Omega}(\mathbf{q}_f, \mathbf{q}_i) \quad , \\ V^{I \left(\begin{smallmatrix} C \\ LS \end{smallmatrix} \right)}(\mathbf{q}_f, \mathbf{q}_i) &= e^{-\frac{3}{32\nu} k^2} \left(\frac{2(1+\xi)^2}{3\pi\nu} \right)^{\frac{3}{2}} \int d\mathbf{p} \exp \left\{ -\frac{2(1+\xi)^2}{3\nu} \left(\mathbf{p} - \frac{1+4\xi}{4(1+\xi)} \mathbf{q} \right)^2 \right\} \\ &\quad \times \left\{ \begin{array}{l} g_0^I \left(\mathbf{p} + \frac{1}{2} \mathbf{k}, \mathbf{p} - \frac{1}{2} \mathbf{k}; (1+\xi) |\mathbf{q} - \mathbf{p}|, \omega \right) \\ h^I \left(\mathbf{p} + \frac{1}{2} \mathbf{k}, \mathbf{p} - \frac{1}{2} \mathbf{k}; (1+\xi) |\mathbf{q} - \mathbf{p}|, \omega \right) i \widehat{[\mathbf{p} \times \mathbf{k}]} \cdot \boldsymbol{\sigma}_1 \end{array} \right\} \quad , \end{aligned} \quad (2.13)$$

where $h^I = h_0^I + h_-^I$ and $\widehat{[\mathbf{p} \times \mathbf{k}]} = [\mathbf{p} \times \mathbf{q}] / |\mathbf{p} \times \mathbf{q}|$.

It should be noted that the c.m. momentum of the two interacting particles, $\mathbf{K} = (1+\xi)(\mathbf{q} - \mathbf{p})$, in Eqs. (2.11) and (2.13) implies that the local momentum $\mathbf{q} = (\mathbf{q}_f + \mathbf{q}_i)/2$ in Eq. (2.12) plays the role of the incident momentum of the first baryon B from Eq. (2.3), and \mathbf{p} the local momentum of the two-particle system, which is now an integral variable. This is a consequence of fixing the c.m. motion of the $B_8\alpha$ system as in Eq. (2.1), and is a special situation of the direct and knock-on (exchange) terms. The G -matrix depends only on the magnitude $K = |\mathbf{K}|$, since we make an angular average in the G -matrix calculation [12,13]. The G -matrix value is, therefore, specified by K and ω , or alternatively by the incident momentum $q_1 = |\mathbf{q}_1|$ and the relative momentum $q = |\mathbf{q}|$ between B and N ; i.e., $G(\mathbf{p}, \mathbf{p}'; K, \omega) = G(\mathbf{q} + \mathbf{k}/2, \mathbf{q} - \mathbf{k}/2; q_1, q)$ with

$\mathbf{k} = \mathbf{p} - \mathbf{p}'$ and $\mathbf{q} = (\mathbf{p} + \mathbf{p}')/2$. If q_1 and q are specified, K is determined by the angular averaging, and q_2 is determined from q_1 and K . Then the starting energy ω is determined as the sum of the relative kinetic energy of two particles and the s.p. potentials for B_8 and N at q_1 and q_2 , respectively. We therefore choose $q_1 = |\mathbf{q}_f + \mathbf{q}_i|/2$ and $q = |\mathbf{p}|$ in the G -matrix in Eqs. (2.11) and (2.13). In order to carry out this rather involved calculation, we will develop in the next subsection some kind of transformation formula for the rearrangement of relative momenta in the partial-wave components of nonlocal kernels.

2.2 A transformation formula of the nonlocal kernel in the momentum representation

The folding formula in Eq. (2.11) implies that expressing the G -matrix interaction $G^C(\mathbf{p}, \mathbf{p}')$ and $G^{LS}(\mathbf{p}, \mathbf{p}') i[\widehat{\mathbf{p}' \times \mathbf{p}}] \cdot \mathbf{S}$ with the subsidiary momentum variables

$$\begin{aligned} \mathbf{k} &= \mathbf{p} - \mathbf{p}' \quad , & \mathbf{p} &= \mathbf{q} + \frac{1}{2}\mathbf{k} \quad , \\ \mathbf{q} &= \frac{1}{2}(\mathbf{p} + \mathbf{p}') \quad , & \mathbf{p}' &= \mathbf{q} - \frac{1}{2}\mathbf{k} \quad , \end{aligned} \quad (2.14)$$

is convenient for the α -cluster folding. We express these kernels using the calligraphic letters; i.e.,

$$\begin{aligned} \mathcal{G}^C(\mathbf{k}, \mathbf{q}) &= G^C(\mathbf{p}, \mathbf{p}') \quad , \\ \mathcal{G}^{LS}(\mathbf{k}, \mathbf{q}) i[\widehat{\mathbf{q} \times \mathbf{k}}] \cdot \mathbf{S} &= G^{LS}(\mathbf{p}, \mathbf{p}') i[\widehat{\mathbf{p}' \times \mathbf{p}}] \cdot \mathbf{S} \quad . \end{aligned} \quad (2.15)$$

By using this notation and the q_1, q notation for K, ω , discussed in the last subsection, G^{space} in Eq. (2.11), for example, becomes $\mathcal{G}^{\text{space}}(\mathbf{k}, \mathbf{p}; q_1, p)$ with $q_1 = |\mathbf{q}_f + \mathbf{q}_i|/2$. In the following, we omit the argument K, ω or q_1, q for simplicity, unless the dependence becomes crucial for the relationship under consideration. After making partial wave decomposition in Eq. (2.15), we can easily carry out the integral over \mathbf{p} . The resultant expression is denoted by $\mathcal{V}^C(\mathbf{k}, \mathbf{q})$ and by $\mathcal{V}^{LS}(\mathbf{k}, \mathbf{q}) i[\widehat{\mathbf{q} \times \mathbf{k}}] \cdot \mathbf{S}$. The desired Born kernels, $V^C(\mathbf{q}_f, \mathbf{q}_i)$ and $V^{LS}(\mathbf{q}_f, \mathbf{q}_i) i[\widehat{\mathbf{q}_i \times \mathbf{q}_f}] \cdot \mathbf{S}$, are obtained from another transformation related to Eq. (2.12).

Our task is, therefore, to relate the partial-wave components $\mathcal{G}_\lambda^C(k, q)$ and $G_\ell^C(p, p')$, and also $\mathcal{G}_\lambda^{LS}(k, q)$ and $G_\ell^{LS}(p, p')$, which are defined through

$$\begin{aligned}
\mathcal{G}^C(\mathbf{k}, \mathbf{q}) &= \sum_{\lambda=0}^{\infty} (2\lambda + 1) \mathcal{G}_{\lambda}^C(k, q) P_{\lambda}(\hat{\mathbf{k}} \cdot \hat{\mathbf{q}}) \ , \\
G^C(\mathbf{p}, \mathbf{p}') &= \sum_{\ell=0}^{\infty} (2\ell + 1) G_{\ell}^C(p, p') P_{\ell}(\hat{\mathbf{p}} \cdot \hat{\mathbf{p}}') \ , \\
\mathcal{G}^{LS}(\mathbf{k}, \mathbf{q}) &= \sum_{\lambda=1}^{\infty} (2\lambda + 1) \mathcal{G}_{\lambda}^{LS}(k, q) P_{\lambda}^1(\hat{\mathbf{k}} \cdot \hat{\mathbf{q}}) \ , \\
G^{LS}(\mathbf{p}, \mathbf{p}') &= \sum_{\ell=1}^{\infty} (2\ell + 1) G_{\ell}^{LS}(p, p') P_{\ell}^1(\hat{\mathbf{p}} \cdot \hat{\mathbf{p}}') \ .
\end{aligned} \tag{2.16}$$

We generalize the transformation Eq. (2.14) as

$$\begin{pmatrix} \mathbf{p} \\ \mathbf{p}' \end{pmatrix} = \begin{pmatrix} \frac{1}{2} & 1 \\ -\frac{1}{2} & 1 \end{pmatrix} \begin{pmatrix} \mathbf{k} \\ \mathbf{q} \end{pmatrix} = \begin{pmatrix} \alpha & \beta \\ \gamma & \delta \end{pmatrix} \begin{pmatrix} \mathbf{k} \\ \mathbf{q} \end{pmatrix} \ , \tag{2.17}$$

with $\alpha\delta - \beta\gamma = 1$. A simple calculation gives

$$\mathcal{G}_{\lambda}^C(k, q) = \sum_{\ell=0}^{\infty} \frac{1}{2} \int_{-1}^1 dx \frac{G_{\ell}^C(p, p')}{(pp')^{\ell}} P_{\lambda}(x) g_{\ell}(k, q; x) \ , \tag{2.18}$$

where $g_{\ell}(k, q; x) = (pp')^{\ell} P_{\ell}(\hat{\mathbf{p}} \cdot \hat{\mathbf{p}}')$ with

$$p = \sqrt{\alpha^2 k^2 + \beta^2 q^2 + 2\alpha\beta kqx} \ , \quad p' = \sqrt{\gamma^2 k^2 + \delta^2 q^2 + 2\gamma\delta kqx} \ . \tag{2.19}$$

The transformation of the LS components is similarly carried out by using the orthogonality relations of $P_{\ell}^1(x)$ and

$$\begin{aligned}
\left(\frac{1}{\sin\theta}\right) P_{\ell}^1(\cos\theta) &= \sum_{\ell'=\ell-1, \ell-3, \dots, 1 \text{ or } 0} (2\ell' + 1) P_{\ell'}(\cos\theta) \ , \\
P_{\lambda-1}(x) - P_{\lambda+1}(x) &= \frac{2\lambda + 1}{\lambda(\lambda + 1)} \sqrt{1 - x^2} P_{\lambda}^1(x) \ .
\end{aligned} \tag{2.20}$$

For the numerical integration over x in Eq. (2.18) etc., it is convenient to use the spline interpolation

$$G_{\ell}^{\Omega}(p, p') = \sum_{i,j} S_i(p) S_j(p') G_{\ell}^{\Omega}(p_i, p_j) \ , \tag{2.21}$$

since the G-matrix calculation itself is very much time consuming. After all, we obtain the following formula for the transformation of the partial-wave components:

$$\begin{aligned}
\mathcal{G}_\lambda^\Omega(k, q) &= \sum_{i,j} \sum_{\ell=0 \text{ or } 1}^{\infty} (2\ell + 1) F_{i,j}^{\Omega\lambda\ell} G_\ell^\Omega(p_i, p_j) \quad (\Omega = C, LS) , \\
F_{i,j}^{C\lambda\ell} &= \frac{1}{2} \int_{-1}^1 dx \frac{S_i(p)S_j(p')}{(pp')^\ell} P_\lambda(x) g_\ell(k, q; x) , \\
F_{i,j}^{LS\lambda\ell} &= \frac{kq}{2\lambda + 1} \sum_{\ell'=\ell-1, \ell-3, \dots, 1 \text{ or } 0} (2\ell' + 1) \frac{1}{2} \int_{-1}^1 dx \frac{S_i(p)S_j(p')}{(pp')^{\ell'+1}} \\
&\quad \times [P_{\lambda-1}(x) - P_{\lambda+1}(x)] g_{\ell'}(k, q; x) , \tag{2.22}
\end{aligned}$$

where

$$\begin{aligned}
g_\ell(k, q; x) &= (pp')^\ell P_\ell(\hat{\mathbf{p}} \cdot \hat{\mathbf{p}}') \\
&= \sum_{\ell_1+\ell_2=\ell} \sum_{\ell_1'+\ell_2'=\ell} (-1)^{\ell_2+\ell_1'} \frac{(2\ell + 1)!}{\sqrt{(2\ell_1)!(2\ell_2)!(2\ell_1')!(2\ell_2')!}} \alpha^{\ell_1} \beta^{\ell_2} \gamma^{\ell_1'} \delta^{\ell_2'} \\
&\quad \times k^{\ell_1+\ell_1'} q^{\ell_2+\ell_2'} \sum_{\ell'} \langle \ell_1 0 \ell_1' 0 | \ell' 0 \rangle \langle \ell_2 0 \ell_2' 0 | \ell' 0 \rangle \begin{Bmatrix} \ell_1 & \ell_2 & \ell \\ \ell_2' & \ell_1' & \ell' \end{Bmatrix} P_{\ell'}(x) . \tag{2.23}
\end{aligned}$$

The summation over ℓ in Eq. (2.22) is from $\ell = 0$ for $\Omega = C$ and from $\ell = 1$ for $\Omega = LS$.

It is important to note some symmetries possessed by $\mathcal{G}_\lambda^\Omega(\mathbf{k}, \mathbf{q})$. From the time-reversal symmetry, the G -matrix $G^\Omega(\mathbf{p}, \mathbf{p}')$ is symmetric for the interchange of \mathbf{p} and \mathbf{p}' . Since this interchange corresponds to $\mathbf{k} \rightarrow -\mathbf{k}$, the transformed partial-wave components, $\mathcal{G}_\lambda^C(k, q)$ and $\mathcal{G}_\lambda^{LS}(k, q)$, are no-zero only for $\lambda = 0, 2, 4, \dots$ and $\lambda = 1, 3, 5, \dots$, respectively. For the coefficients in Eq. (2.17), we can show $g_\ell(2q, k/2; x) = (-1)^\ell g_\ell(k, q; x)$ in Eq. (2.23). This property implies that, if $G_\ell^\Omega(p, p')$ is transformed to $\mathcal{G}_\lambda^\Omega(k, q)$, then $(-1)^\ell G_\ell^\Omega(p, p')$ is transformed to $\mathcal{G}_\lambda^\Omega(2q, k/2)$. In the later application of the present formalism to $n\alpha$ resonating-group method (RGM), we will find that the knock-on term is obtained by simply replacing $\mathcal{G}_\lambda^\Omega(k, q)$ to $\mathcal{G}_\lambda^\Omega(2q, k/2)$ in the direct term. In fact, the knock-on term is already included even in the hyperon α system as in Eq. (2.4), which is the strangeness exchange term of the hyperon-nucleon interaction. In other words, the direct and knock-on terms are treated on the equal footing in the present formalism to deal with the invariant G -matrix interaction. For the transformation from $\mathcal{V}^\Omega(\mathbf{k}, \mathbf{q})$ to $V^\Omega(\mathbf{q}_f, \mathbf{q}_i)$, we find that the latter Born kernel is symmetric with respect to the interchange of q_f and q_i , which is the consequence of Eqs. (2.19) and (2.22) for the transformation coefficients (see Eq. (2.12))

$$\begin{pmatrix} \mathbf{k} \\ \mathbf{q} \end{pmatrix} = \begin{pmatrix} 1 & -1 \\ \frac{1}{2} & \frac{1}{2} \end{pmatrix} \begin{pmatrix} \mathbf{q}_f \\ \mathbf{q}_i \end{pmatrix} . \tag{2.24}$$

2.3 Partial-wave expansion of the $B_8\alpha$ Born kernel

If we use partial-wave decomposition in Eq. (2.16) and the similar expansions for $\mathcal{V}^\Omega(\mathbf{k}, \mathbf{q}) = V^\Omega(\mathbf{q}_f, \mathbf{q}_i)$, the folding formula Eq. (2.11) becomes very simple. For both of the $\Omega = C$ and LS terms, it is given by

$$\begin{aligned} \mathcal{V}_\lambda^\Omega(k, q) &= \exp \left\{ -\frac{3}{32\nu} k^2 - \frac{2}{3\nu} \left(\frac{1}{4} + \xi \right)^2 q^2 \right\} \left(\frac{2(1+\xi)^2}{3\pi\nu} \right)^{\frac{3}{2}} 4\pi \\ &\times \int_0^\infty p^2 dp \exp \left\{ -\frac{2(1+\xi)^2}{3\nu} p^2 \right\} i_\lambda \left(\frac{(1+\xi)(1+4\xi)}{3\nu} pq \right) \mathcal{G}_\lambda^\Omega(k, p) \quad , \end{aligned} \quad (2.25)$$

where $i_\lambda(x) = i^\lambda j_\lambda(-ix)$ is the spherical Bessel function of the imaginary argument. For the proof of the LS -term folding, we use a simple formula

$$P_\ell^1(\hat{\mathbf{k}} \cdot \hat{\mathbf{q}}) i[\widehat{\mathbf{q} \times \mathbf{k}}]_\nu = (-1)^\ell \frac{4\pi}{\sqrt{3}} \sqrt{\frac{\ell(\ell+1)}{2\ell+1}} [Y_\ell(\hat{\mathbf{k}}) Y_\ell(\hat{\mathbf{q}})]_{1\nu} \quad , \quad (2.26)$$

which is derived by using

$$P_{\ell+1}^1(x) - P_{\ell-1}^1(x) = (2\ell+1) \sqrt{1-x^2} P_\ell(x) \quad , \quad (2.27)$$

and

$$\begin{aligned} P_\ell(\hat{\mathbf{k}} \cdot \hat{\mathbf{q}}) i[\mathbf{q} \times \mathbf{k}]_\nu &= (-1)^\ell \frac{4\pi}{\sqrt{3}} \frac{kq}{(2\ell+1)} \left\{ \sqrt{\frac{(\ell+1)(\ell+2)}{2\ell+3}} \right. \\ &\times \left. [Y_{\ell+1}(\hat{\mathbf{q}}) Y_{\ell+1}(\hat{\mathbf{k}})]_{1\nu} - \sqrt{\frac{(\ell-1)\ell}{2\ell-1}} [Y_{\ell-1}(\hat{\mathbf{q}}) Y_{\ell-1}(\hat{\mathbf{k}})]_{1\nu} \right\} \quad . \end{aligned} \quad (2.28)$$

The final step to derive the partial-wave components $V_\ell^\Omega(q_f, q_i)$ in

$$\begin{aligned} V(\mathbf{q}_f, \mathbf{q}_i) &= V^C(\mathbf{q}_f, \mathbf{q}_i) + V^{LS}(\mathbf{q}_f, \mathbf{q}_i) i[\widehat{\mathbf{q}_i \times \mathbf{q}_f}] \cdot \mathbf{S} \quad , \\ V^C(\mathbf{q}_f, \mathbf{q}_i) &= \sum_{\ell=0}^{\infty} (2\ell+1) V_\ell^C(q_f, q_i) P_\ell(\hat{\mathbf{q}}_f \cdot \hat{\mathbf{q}}_i) \quad , \\ V^{LS}(\mathbf{q}_f, \mathbf{q}_i) &= \sum_{\ell=1}^{\infty} (2\ell+1) V_\ell^{LS}(q_f, q_i) P_\ell^1(\hat{\mathbf{q}}_f \cdot \hat{\mathbf{q}}_i) \quad , \end{aligned} \quad (2.29)$$

is carried out by using the transformation formula in the preceding subsection with the coefficients in Eq. (2.24). In the jj -coupling scheme, we also need

$V_\ell^J(q_f, q_i)$ in the partial-wave expansion

$$V(\mathbf{q}_f, \mathbf{q}_i) = 4\pi \sum_{J\ell} V_\ell^J(q_f, q_i) \sum_M \mathcal{Y}_{(\ell\frac{1}{2})JM}(\hat{\mathbf{q}}_f; \text{spin}) \mathcal{Y}_{(\ell\frac{1}{2})JM}^*(\hat{\mathbf{q}}_i; \text{spin}) \quad ,$$

which is given by

$$\begin{aligned} V_\ell^J(q_f, q_i) &= V_\ell^C(q_f, q_i) + V_\ell^{LS}(q_f, q_i) \langle \mathbf{L} \cdot \mathbf{S} \rangle_{J\ell} \quad , \\ \langle \mathbf{L} \cdot \mathbf{S} \rangle_{J\ell} &= \frac{1}{2} \left[J(J+1) - \ell(\ell+1) - \frac{3}{4} \right] = \begin{cases} \frac{\ell}{2} & \text{for } J = \begin{cases} \ell + \frac{1}{2} \\ \ell - \frac{1}{2} \end{cases} \\ -\frac{\ell+1}{2} & \end{cases} \quad . \end{aligned} \quad (2.30)$$

In Eq. (2.30), $\mathcal{Y}_{(\ell\frac{1}{2})JM}(\hat{\mathbf{q}}; \text{spin}) = [Y_\ell(\hat{\mathbf{q}}) \chi_{\frac{1}{2}}]_{JM}$ is the angular-spin wave function of the $B_8\alpha$ system. For the proof, we again use Eq. (2.26).

In summary, the Born kernel of the $B_8\alpha$ system is obtained by using Eqs. (2.22) and (2.25), starting from

$$\begin{aligned} G_\ell^C(p, p') &= \frac{1}{2} \sum_{IJS} \left(\frac{2I+1}{2I_B+1} \right) \left(\frac{2J+1}{2\ell+1} \right) G_{S\ell, S\ell}^{IJ}(p, p') \quad (\ell = 0, 1, 2, \dots) \quad , \\ G_\ell^{LS}(p, p') &= \sum_I \left(\frac{2I+1}{2I_B+1} \right) \left\{ -\frac{1}{\ell(\ell+1)} G_{1\ell, 1\ell}^{I\ell}(p, p') - \frac{2\ell-1}{\ell(2\ell+1)} G_{1\ell, 1\ell}^{I\ell-1}(p, p') \right. \\ &\quad \left. + \frac{2\ell+3}{(\ell+1)(2\ell+1)} G_{1\ell, 1\ell}^{I\ell+1}(p, p') + \frac{1}{\sqrt{\ell(\ell+1)}} \left[G_{1\ell, 0\ell}^{I\ell}(p, p') + G_{0\ell, 1\ell}^{I\ell}(p, p') \right] \right\} \\ &\quad (\ell = 1, 2, 3, \dots) \quad . \quad (2.31) \end{aligned}$$

For $B_8 = N$, we should multiply the factor 2 to include the knock-on term. We first use Eq. (2.22) with the coefficients Eq. (2.17) and transform the above $G_\ell^\Omega(p, p')$ to $\mathcal{G}_\lambda^\Omega(k, q)$. Then, the α -cluster folding by Eq. (2.25) yields $\mathcal{V}_\lambda^\Omega(k, q)$ from $\mathcal{G}_\lambda^\Omega(k, q)$. The second transformation from $\mathcal{V}_\lambda^\Omega(k, q)$ to $V_\lambda^\Omega(q_f, q_i)$ is carried out with the coefficient Eq. (2.24). The selection of q_1 and q in $G^\Omega(p, p'; q_1, q)$ is now almost apparent. We choose q_1 as q in the folding formula Eq. (2.25). The relative momentum q is actually p in Eq. (2.25). Therefore, the nest structure $\mathcal{V}_\lambda^\Omega(k, q) \supset \mathcal{G}_\lambda^\Omega(k, p; q_1 = q, q = p)$ and $\mathcal{G}_\lambda^\Omega(k, q; q_1, q) \supset G_\ell^\Omega(p, p'; q_1, q)$ is incorporated in the computer code. Namely, we first specify k and q in Eq. (2.25). Then $\mathcal{G}_\lambda^\Omega(k, p; q_1 = q, q = p)$ is generated from $\mathcal{G}_\lambda^\Omega(k, q; q_1, q)$ for a general q , which is obtained from the transformation formula, Eq. (2.22), by using the complete off-shell G -matrix $G_\ell^\Omega(p_i, p_j; q_1, q)$.

2.4 Wigner transform

The present formalism is convenient to calculate the Wigner transform $V_W^\Omega(\mathbf{r}, \mathbf{q})$, since they are essentially the Fourier transform of $\mathcal{V}^\Omega(\mathbf{k}, \mathbf{q})$. We define these through

$$\begin{aligned} V_W(\mathbf{r}, \mathbf{q}) &= \frac{1}{(2\pi)^3} \int d\mathbf{k} e^{i\mathbf{k}\cdot\mathbf{r}} V(\mathbf{q} + \mathbf{k}/2, \mathbf{q} - \mathbf{k}/2) \\ &= \frac{1}{(2\pi)^3} \int d\mathbf{k} e^{i\mathbf{k}\cdot\mathbf{r}} \left\{ \mathcal{V}^C(\mathbf{k}, \mathbf{q}) + \mathcal{V}^{LS}(\mathbf{k}, \mathbf{q}) i[\widehat{\mathbf{q} \times \mathbf{k}}] \cdot \mathbf{S} \right\} \\ &= V_W^C(\mathbf{r}, \mathbf{q}) + V_W^{LS}(\mathbf{r}, \mathbf{q}) [\mathbf{r} \times \mathbf{q}] \cdot \mathbf{S} . \end{aligned} \quad (2.32)$$

Note that the LS term is defined by $\mathbf{L}_W \cdot \mathbf{S} \equiv [\mathbf{r} \times \mathbf{q}] \cdot \mathbf{S}$, instead of $i[\widehat{\mathbf{r} \times \mathbf{q}}] \cdot \mathbf{S}$. If we apply the partial-wave expansion

$$\begin{aligned} V_W^C(\mathbf{r}, \mathbf{q}) &= \sum_{\lambda=0}^{\infty} (2\lambda + 1) V_{W\lambda}^C(r, q) P_\lambda(\cos \varphi) , \\ V_W^{LS}(\mathbf{r}, \mathbf{q}) &= \sum_{\lambda=1}^{\infty} (2\lambda + 1) V_{W\lambda}^{LS}(r, q) \left(\frac{1}{\sin \varphi} \right) P_\lambda^1(\cos \varphi) , \end{aligned} \quad (2.33)$$

with $\cos \varphi = (\hat{\mathbf{r}} \cdot \hat{\mathbf{q}})$, we can easily derive the partial-wave components as

$$\begin{aligned} V_{W\lambda}^C(r, q) &= \frac{4\pi}{(2\pi)^3} \int_0^\infty k^2 dk i^\lambda j_\lambda(kr) \mathcal{V}_\lambda^C(k, q) , \\ V_{W\lambda}^{LS}(r, q) &= \frac{1}{qr} \frac{4\pi}{(2\pi)^3} \int_0^\infty k^2 dk i^{\lambda-1} j_\lambda(kr) \mathcal{V}_\lambda^{LS}(k, q) . \end{aligned} \quad (2.34)$$

Here we use Eq. (2.26) again for the derivation of the LS term. Since $V_{W\lambda}^C(r, q) \neq 0$ for $\lambda = 0, 2, 4, \dots$ and $V_{W\lambda}^{LS}(r, q) \neq 0$ for $\lambda = 1, 3, 5, \dots$ (see Subsec. 2.2), the $\lambda = 0$ and $\lambda = 1$ terms become the leading terms for the central and LS Wigner transform, respectively. In fact, in the $q = 0$ case, we find that only these leading terms survive for the zero-momentum Wigner transform. It is, therefore, a good approximation to retain only $\lambda = 0$ and $\lambda = 1$ terms in Eq. (2.33):

$$\begin{aligned} V_W^C(\mathbf{r}, \mathbf{q}) &\sim \frac{4\pi}{(2\pi)^3} \int_0^\infty k^2 dk j_0(kr) \mathcal{V}_0^C(k, q) , \\ V_W^{LS}(\mathbf{r}, \mathbf{q}) &\sim \frac{4\pi}{(2\pi)^3} \int_0^\infty k^2 dk \frac{1}{r} j_1(kr) \frac{3}{q} \mathcal{V}_1^{LS}(k, q) , \end{aligned} \quad (2.35)$$

which we use throughout this paper.

The zero-momentum Wigner transform is a convenient tool to estimate the strength of the interaction. From the folding formula Eq. (2.25), we can calculate $\mathcal{V}_0^C(k, 0)$ and $(3/q)\mathcal{V}_1^{LS}(k, q)|_{q=0}$. This process yields

$$\begin{aligned}
V_W^C(\mathbf{r}, 0) &= \frac{2}{\pi} \int_0^\infty k^2 dk e^{-\frac{3}{32\nu}k^2} j_0(kr) \\
&\quad \times \left(\frac{2(1+\xi)^2}{3\pi\nu} \right)^{\frac{3}{2}} \int_0^\infty q^2 dq e^{-\frac{2(1+\xi)^2}{3\nu}q^2} \mathcal{G}_0^C(k, q) \ , \\
V_W^{LS}(\mathbf{r}, 0) &= \frac{(1+\xi)(1+4\xi)}{3\nu} \frac{2}{\pi} \int_0^\infty k^2 dk e^{-\frac{3}{32\nu}k^2} \frac{1}{r} j_1(kr) \\
&\quad \times \left(\frac{2(1+\xi)^2}{3\pi\nu} \right)^{\frac{3}{2}} \int_0^\infty q^3 dq e^{-\frac{2(1+\xi)^2}{3\nu}q^2} \mathcal{G}_1^{LS}(k, q) \ .
\end{aligned} \tag{2.36}$$

For the LS component, it is easy to introduce another approximation, which gives a simple factor for the LS strength, similar to the Scheerbaum's factor [19]. For this purpose, we express $\mathcal{G}_1^{LS}(k, q)$ in the original form

$$\begin{aligned}
\mathcal{G}_1^{LS}(k, q) &= \frac{kq}{3} \sum_{\ell=1}^{\infty} (2\ell+1) \frac{1}{2} \int_{-1}^1 dx [1 - P_2(x)] \frac{G_\ell^{LS}(p, p')}{pp'} \\
&\quad \times \left(\frac{1}{\sin \theta} \right) P_\ell^1(\cos \theta) \ ,
\end{aligned} \tag{2.37}$$

where $\cos \theta = (\hat{\mathbf{p}} \cdot \hat{\mathbf{p}}')$ with $\mathbf{p} = \mathbf{q} + \mathbf{k}/2$, $\mathbf{p}' = \mathbf{q} - \mathbf{k}/2$ and $x = (\hat{\mathbf{k}} \cdot \hat{\mathbf{q}})$. We neglect the k dependence except for the front factor $kq/3$ and set $k = 0$. Then, $p, p' \rightarrow q$, $\cos \theta \rightarrow 1$, and the x integral can be performed. By further using $P_\ell'(1) = \ell(\ell+1)/2$, we obtain

$$\begin{aligned}
\mathcal{G}_1^{LS}(k, q) &\sim \frac{kq}{3} \sum_{\ell=1}^{\infty} (2\ell+1) \frac{1}{q^2} G_\ell^{LS}(q, q) \frac{\ell(\ell+1)}{2} \\
&= \left(\frac{2k}{3q} \right) \frac{1}{4} \sum_{\ell=1}^{\infty} \ell(\ell+1)(2\ell+1) G_\ell^{LS}(q, q) \ .
\end{aligned} \tag{2.38}$$

If we set

$$\begin{aligned}
G(q) &= \frac{1}{4} \sum_{\ell=1}^{\infty} \ell(\ell+1)(2\ell+1) G_{\ell}^{LS}(q, q) \\
&= \frac{1}{4} \sum_{IJ} \left(\frac{2I+1}{2I_B+1} \right) (2J+1) \left\{ -G_{1J,1J}^{IJ}(q, q) - (J+2)G_{1J+1,1J+1}^{IJ}(q, q) \right. \\
&\quad \left. + (J-1)G_{1J-1,1J-1}^{IJ}(q, q) + \sqrt{J(J+1)} \left[G_{1J,0J}^{IJ}(q, q) + G_{0J,1J}^{IJ}(q, q) \right] \right\} \\
&= 2 \sum_{IJ} \left(\frac{2I+1}{2I_B+1} \right) \left[h_0^I(\mathbf{p}, \mathbf{p}') + h_-^I(\mathbf{p}, \mathbf{p}') \right] \frac{1}{\sin \theta} \Big|_{\mathbf{p}=\mathbf{p}'=\mathbf{q}} , \quad (2.39)
\end{aligned}$$

we can write $\mathcal{G}_1^{LS}(k, q) \sim (2k/3q)G(q)$. Using this and the integration formula

$$\frac{2}{\pi} \int_0^{\infty} k^3 dk e^{-\frac{3}{32\nu}k^2} \frac{1}{r} j_1(kr) = \frac{8}{\sqrt{\pi}} \left(\frac{8\nu}{3} \right)^{\frac{5}{2}} e^{-\frac{8}{3}\nu r^2} , \quad (2.40)$$

we find

$$\begin{aligned}
V_W^{LS}(\mathbf{r}, 0) &\sim \frac{2}{3} \frac{(1+\xi)(1+4\xi)}{3\nu} \frac{8}{\sqrt{\pi}} \left(\frac{8\nu}{3} \right)^{\frac{5}{2}} e^{-\frac{8}{3}\nu r^2} \\
&\quad \times \left(\frac{2(1+\xi)^2}{3\pi\nu} \right)^{\frac{3}{2}} \int_0^{\infty} q^2 dq e^{-\frac{2(1+\xi)^2}{3\nu}q^2} G(q) . \quad (2.41)
\end{aligned}$$

We can write Eq. (2.41) in the way similar to the Scheerbaum's formula:

$$U(r) = -\frac{\pi}{2} S_B \frac{1}{r} \frac{d\rho(r)}{dr} \boldsymbol{\ell} \cdot \boldsymbol{\sigma} . \quad (2.42)$$

For the $B_8\alpha$ system, the density $\rho(r)$ of the α -cluster is calculated as

$$\rho(r) = \langle \phi_{\alpha} | \sum_{i=1}^4 \delta(\mathbf{r} - \boldsymbol{\xi}_i) | \phi_{\alpha} \rangle = 4 \left(\frac{8\nu}{3\pi} \right)^{\frac{3}{2}} e^{-\frac{8}{3}\nu r^2} , \quad (2.43)$$

where $\boldsymbol{\xi}_i = \mathbf{x}_i - \mathbf{X}_{\alpha}$ is the coordinate of the nucleon i , measured from the c.m. of the α -cluster. Then, we find that the integral Eq. (2.40) is nothing but $(-\pi)(1/r)(d\rho(r)/dr)$. Thus Eq. (2.42) becomes

$$U(r) = S_B \frac{8}{\sqrt{\pi}} \left(\frac{8\nu}{3} \right)^{\frac{5}{2}} e^{-\frac{8}{3}\nu r^2} \boldsymbol{\ell} \cdot \mathbf{S} . \quad (2.44)$$

Similarly, we can write Eq. (2.41) as

$$V_W^{LS}(\mathbf{r}, 0) = \tilde{S}_B \frac{8}{\sqrt{\pi}} \left(\frac{8\nu}{3} \right)^{\frac{5}{2}} e^{-\frac{8}{3}\nu r^2} , \quad (2.45)$$

and obtain

$$\tilde{S}_B = \frac{1+4\xi}{4\xi} \frac{1}{2\pi} \frac{\xi}{1+\xi} \frac{8\pi^2}{3} \left(\frac{2(1+\xi)^2}{3\pi\nu} \right)^{\frac{5}{2}} \int_0^{\infty} q^2 dq e^{-\frac{2(1+\xi)^2}{3\nu}q^2} G(q) . \quad (2.46)$$

This expression corresponds to Eq. (50) of Ref. [13], which is the Scheerbaum factor of finite nuclei derived from G -matrix calculations:

$$S_B(q_1) = \frac{1}{2\pi} \frac{\xi}{1+\xi} \frac{3}{(k_F)^3} (1+\xi)^3 \int_0^{q_{\max}} dq W(q_1, q) G(q) . \quad (2.47)$$

The difference between Eqs. (2.46) and (2.47) is the weight function,

$$W(q) = q^2 e^{-\frac{2(1+\xi)^2}{3\nu} q^2} \longleftrightarrow W(q_1, q) , \quad (2.48)$$

and an extra front factor $\frac{1+4\xi}{4\xi}$ in Eq. (2.46). This enhancement factor appears, since in the standard G -matrix calculation of single-particle potentials the c.m. motion of the total system is not correctly treated. In the $B_8\alpha$ system, this approximation affects the result appreciably, which is discussed in Ref. [8]. The two weight functions in Eq. (2.48) may seem to be fairly different, since $W(q_1, q)$ with $q_1 = 0$ is given by $W(0, q) = \theta(q - k_F/(1+\xi))$. However, this is not the case, since in the small q region (the low-energy region) $G(q)$ is anyway very small. We can further approximate Eqs. (2.46) and (2.47), by calculating $\bar{q} = \sqrt{\langle q^2 \rangle}$ with each weight function, and by replacing q in $G(q)$ with this \bar{q} . The average momentum \bar{q} is given by

$$\bar{q} = \frac{3\sqrt{\nu}}{2} \left(\frac{1}{1+\xi} \right) \quad \text{for } W(q) , \quad \bar{q} = \frac{k_F}{\sqrt{3}} \left(\frac{1}{1+\xi} \right) \quad \text{for } W(0, q) . \quad (2.49)$$

For $W(q)$ with $\nu = 0.257 \text{ fm}^{-1}$, $\bar{q} \sim 0.38 \text{ fm}^{-1}$, and for $W(0, q_1)$ with $k_F = 1.2 \text{ fm}^{-1}$, $\bar{q} \sim 0.34 \text{ fm}^{-1}$. These values are very close to $q = \bar{k}/2 = 0.35 \text{ fm}^{-1}$, calculated from the Scheerbaum's estimation for an average momentum transfer $\bar{k} \sim 0.7 \text{ fm}^{-1}$. From this prescription, \tilde{S}_B and $S_B(0)$ are given by

$$\tilde{S}_B = \frac{1+4\xi}{4\xi} \frac{1}{2\pi} \frac{\xi}{1+\xi} \frac{1}{\bar{q}^2} G(\bar{q}) , \quad S_B(0) = \frac{1}{2\pi} \frac{\xi}{1+\xi} \frac{1}{\bar{q}^2} G(\bar{q}) . \quad (2.50)$$

3 Result and discussion

3.1 $\Lambda\alpha$ interaction

In order to gain the overview of the zero-momentum Wigner transform given in Eq. (2.36), we will show in Fig. 1 the central ($V_W^C(\mathbf{r}, 0)$) and LS ($V_W^{LS}(\mathbf{r}, 0)$) components for the $B_8\alpha$ interaction with $B_8 = N, \Lambda, \Sigma$ and Ξ , when the quark-model G -matrix B_8B_8 interaction by fss2 are employed with the continuous choice for intermediate spectra. In this case, we choose $q_1 = 0$ and the relative momentum q is assigned to the integral mesh point q in Eq. (2.36). The Fermi-momentum used for the G -matrix calculation is $k_F = 1.35 \text{ fm}^{-1}$, and the $(0s)^4$ shell-model wave function with the h.o. size parameter $\nu = 0.257 \text{ fm}^{-2}$ is

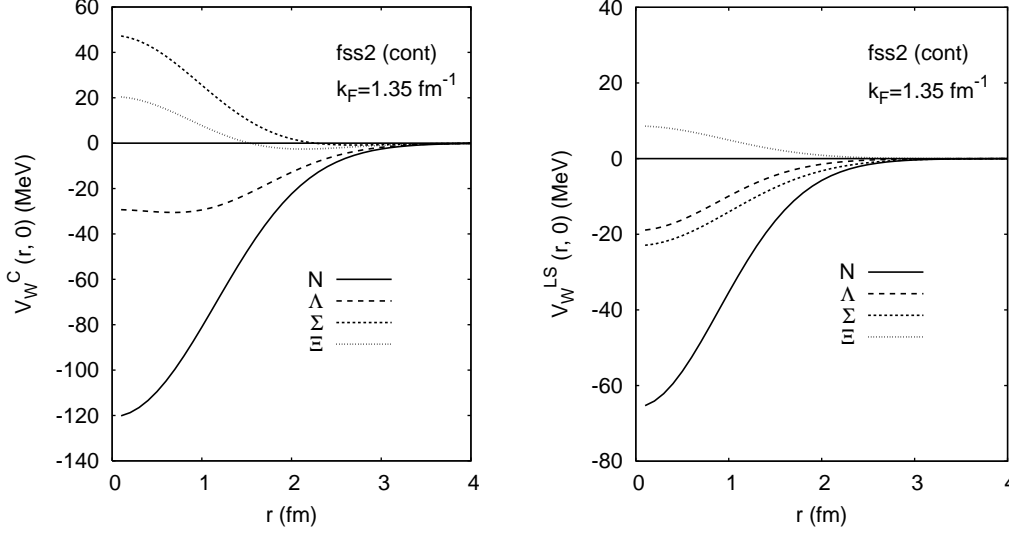


Fig. 1. The central component of the zero-momentum Wigner transform $V_W^C(r, 0)$ for the $B_8\alpha$ Born kernel, calculated from the quark-model G -matrix B_8B_8 interactions by fss2. The Fermi momentum used in the G -matrix calculation is $k_F = 1.35 \text{ fm}^{-1}$ and the continuous choice is used for intermediate spectra. The $(0s)^4$ shell-model wave function with the h.o. size parameter $\nu = 0.257 \text{ fm}^{-2}$ is used for the α cluster.

used for the α -cluster folding. We note that the correct treatment of the total c.m. motion for the $B_8\alpha$ system is very important, since the c.m. correction in the standard approach is of the order of $1/A \sim 1/4$. As the result, the zero-momentum Wigner transform becomes very much short-ranged and deep with the interaction range about $R = 1.2A^{1/3} \sim 2 \text{ fm}$. The α -particle density in Eq. (2.43) is more compact than the density by the standard expression, $\rho(r) = 4(2\nu/\pi)^{3/4} e^{-2\nu r^2}$, and the central density is about $(4/3)^{3/2} \sim 1.5$ times larger. The extremely large $N\alpha$ Wigner transform in Fig. 1 is because of the factor 2 in Eq. (A.9), and also because the other nucleon-exchange term than the knock-on term and the effect of the exchange normalization kernel are neglected. We will deal with this case in a separate paper.

We list in Table 1 the values of the zero-momentum Wigner transform at the origin $\mathbf{r} = 0$, and the Scheerbaum-like factor \tilde{S}_B in Eq. (2.46) for all the possible combinations of G -matrix calculations for the models, fss2 and FSS, and for the QTQ and continuous choices for intermediate spectra. The corresponding values for the single-particle potentials, $U_B(q_1)$, and the Scheerbaum factors, $S_B(q_1)$, at $q_1 = 0$ in symmetric nuclear matter with $k_F = 1.35 \text{ fm}^{-1}$ are listed in Table 2. By comparing these results, we obtain the following findings:

Table 1

Values of the zero-momentum Wigner transform at the origin $\mathbf{r} = 0$, $V_W^C(0, 0)$ and $V_W^{LS}(0, 0)$, and the Scheerbaum-like factor, \tilde{S}_B , in Eq. (2.46). The unit is in MeV for $V_W^C(0, 0)$ and $V_W^{LS}(0, 0)$, and in MeV fm⁵ for \tilde{S}_B . The models are fss2 and FSS, and *qtq* and *cont.* imply the *QTQ* and continuous choices for intermediate spectra, respectively, used in the *G*-matrix calculations.

	<i>B</i>	FSS		fss2	
		<i>qtq</i>	<i>cont</i>	<i>qtq</i>	<i>cont</i>
$V_W^C(0, 0)$	<i>N</i>	-112.8	-121.1	-112.6	-120.0
	Λ	-26.01	-26.03	-28.09	-29.31
	Σ	59.33	48.72	51.76	47.24
	Ξ	7.97	10.73	20.83	20.38
$V_W^{LS}(0, 0)$	<i>N</i>	-65.60	-67.65	-63.89	-65.31
	Λ	-14.54	-14.70	-17.89	-18.91
	Σ	-28.07	-23.45	-24.32	-22.92
	Ξ	18.59	25.55	7.71	8.59
\tilde{S}_B	<i>N</i>	-51.00	-52.24	-52.15	-53.49
	Λ	-5.32	-5.04	-13.22	-13.96
	Σ	-34.87	-30.36	-31.69	-30.89
	Ξ	20.15	26.30	6.77	7.62

1. The $\Lambda\alpha$ central Wigner transforms are fairly shallow in comparison with $U_\Lambda(0)$ in the symmetric nuclear matter calculations. Namely, $|V_W^C(0, 0)|$ is less than 30 MeV in all the cases, while $|U_\Lambda(0)|$ is more than 40 MeV.
2. The $\Sigma\alpha$ and $\Xi\alpha$ central Wigner transforms are repulsive, although $U_\Xi(0)$ is attractive. In particular, $V_W^C(0, 0)$ for $\Sigma\alpha$ is strongly repulsive, which is due to the quark-model prediction of the repulsive $\Sigma N(I = 3/2) {}^3S_1$ interaction. These characters are the result of strong isospin dependence of the ΣN and ΞN interactions, which is discussed in the next subsection.
3. The *LS* component, $V_W^{LS}(0, 0)$, for the $\Lambda\alpha$ interaction is by no means extremely small, in comparison with that for the $\Sigma\alpha$ interaction. The ratio is only 70 – 80 % for fss2 and 50 – 60 % for FSS. On the other hand, \tilde{S}_B factors reflect the characteristics of $S_B(0)$; namely, \tilde{S}_B is about 20 – 30 % larger than $S_B(0)$, which is about equal to the enhancement factor $\frac{1+4\xi}{4\xi} \sim 1.25 - 1.35$ in Eqs. (2.46) and (2.50).

We find that the zero-momentum Wigner transform is not good enough to define phase-shift equivalent local potentials, especially for the $\Lambda\alpha$ interaction, In order to see this clearly, we examined the Wigner transform for several effective $\Lambda\alpha$ potentials, which can be easily derived from the $\Lambda\alpha$ Born kernels given in Appendix B of Ref. [7]. The effective ΛN potentials we examined are

Table 2

The depth of the single-particle potentials, $U_B(q_1)$, and the Scheerbaum factors, $S_B(q_1)$, at $q_1 = 0$ obtained by the angular-averaged G -matrix calculations of the quark-model potentials in symmetric nuclear matter. The Fermi-momentum $k_F = 1.35 \text{ fm}^{-1}$ is used. The models are fss2 and FSS, and qtq and cont. imply the QTQ and continuous choices for intermediate spectra, respectively.

	B	FSS		fss2	
		qtq	cont	qtq	cont
$U_B(0)$	N	-79.8	-89.3	-80.6	-88.9
	Λ	-42.8	-46.3	-44.8	-48.4
	Σ	16.1	17.3	9.5	7.3
	Ξ	-14.9	-20.8	-5.3	-8.2
$S_B(0)$	N	-40.3	-41.4	-41.3	-42.4
	Λ	-3.9	-3.6	-10.0	-10.6
	Σ	-27.4	-22.6	-24.1	-23.2
	Ξ	14.6	21.4	4.6	5.8

the Sparenberg-Baye potential (SB potential) [7] given by

$$v_{\Lambda N} = \left[v(^1E) \frac{1 - P_\sigma}{2} + v(^3E) \frac{1 + P_\sigma}{2} \right] \left[\frac{u}{2} + \frac{2 - u}{2} P_r \right], \quad (3.1)$$

with

$$\begin{aligned} v(^1E) &= -128.0 \exp(-0.8908 r^2) + 1015 \exp(-5.383 r^2), \\ v(^3E) &= -56.31 f \exp(-0.7517 r^2) + 1072 \exp(-13.74 r^2), \end{aligned} \quad (3.2)$$

and the G -matrix simulated ΛN forces [18] generated from the various OBEP potentials, NS (Nijmegen soft-core model NSC89), ND (hard-core model D), NF (hard-core model F), JA (Jülich model A), and JB (model B). By choosing the parameters, $u = 0.94687$ and $f = 0.8923$ in Eqs. (3.1) and (3.2), we can correctly reproduce the Λ separation energy in ${}^5_\Lambda\text{He}$: $E_B^{\text{exp}}({}^5_\Lambda\text{He}) = -3.12 \pm 0.02 \text{ MeV}$. The strength of the short-range repulsive term (the third component) of the NS - JB potentials are slightly modified from the original values, in order to reproduce this value. (See Ref. [7].) The phase-shift equivalent local potential in the semi-classical RGM-WKB approximation [22,23,20] is calculated by solving the transcendental equation

$$U_{\text{eff}}(R) = G^W \left(R, \sqrt{(2\mu_{\Lambda\alpha}/\hbar^2) [E - U_{\text{eff}}(R)]} \right), \quad (3.3)$$

for some specific energies E , where $G^W(R, q)$ is assigned to $V_W^C(\mathbf{r}, \mathbf{q})$ in Eq. (2.35) with $R = r = |\mathbf{r}|$ and $q = |\mathbf{q}|$.² We here study only the S wave, by neglecting

² For the effective ΛN forces, the approximate formula Eq. (2.35) gives an exact

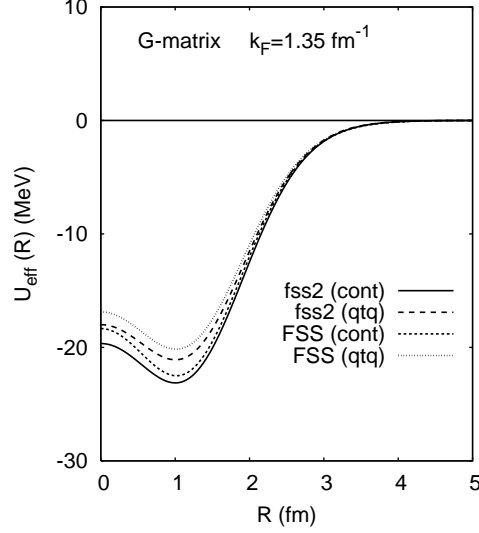
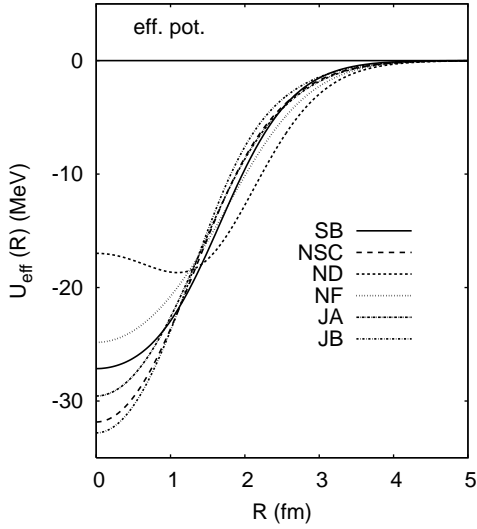


Fig. 3. Solutions of the transcendental equation Eq. (3.3), obtained from the $\Lambda\alpha$ Wigner transform for the various effective ΛN potentials. SB is the Sparenberg-Baye potential, Eqs. (3.1) and (3.2), NSC, ND, NF are the simulated versions of the Nijmegen potentials, and JA, JB are those of the Jülich potentials. The energy $E = -3.12$ MeV is assumed. The $(0s)^4$ shell-model wave function with the h.o. size parameter $\nu = 0.257$ fm $^{-2}$ is used for the α -cluster.

Fig. 4. The same as Fig. 3, but for the Wigner transform, $V_W^C(\mathbf{r}, \mathbf{q})$ in Eq. (2.35), calculated from the quark-model G -matrix interactions. The $\Lambda\alpha$ Born kernels are calculated from the quark-model G -matrix $B_8 B_8$ interactions by fss2 and FSS. The Fermi momentum used in the G -matrix calculation is $k_F = 1.35$ fm $^{-1}$, and qtq stands for the QTQ prescription and $cont$ for the continuous choice for intermediate spectra.

the usual semi-classical centrifugal term $\hbar^2(\ell + 1/2)^2/2\mu_{\Lambda\alpha}$. The centrifugal potentials are included only in the Schrödinger equation. This is a plausible approximation, since the LS term of the $\Lambda\alpha$ interaction is very small. The obtained $\Lambda\alpha$ effective local potentials with $E = -3.12$ MeV are plotted in Fig. 3 for SB - JA potentials. The depth of U_{eff} is tabulated in Table 3, together with the q^2 value at $R = 0$, determined self-consistently. The bound-state energy of this effective local potential, E_B , is calculated by solving the Schrödinger equation

$$\left[-\frac{\hbar^2}{2\mu_{\Lambda\alpha}} \frac{\partial^2}{(\partial R)^2} + U_{\text{eff}}(R) \right] \Psi(R) = E_B \Psi(R) . \quad (3.4)$$

We find that the bound-state energies of SB - JA potentials are too small, compared with the exact value $E_B(\text{exact})$, which is obtained by solving the Lippmann-Schwinger equation using the $\Lambda\alpha$ Born kernels. Namely, E_B from $U_{\text{eff}}(R)$ is from 1.3 MeV to 1.7 MeV too small in magnitude, except for the rather moderate difference 0.74 MeV in ND. Figure 3 shows that this difference is related with the interaction range of $U_{\text{eff}}(R)$; i.e., the range of ND is long result, since $\mathcal{V}_\ell^C(k, q)$ are ℓ independent.

Table 3

The depth of the effective local potential $U_{\text{eff}}(0)$, obtained by solving the transcendental equation Eq. (3.3) with $E = -3.12$ MeV. The q^2 value at $R = 0$ and a special value $V_W^C(0,0)$ of the $\Lambda\alpha$ Wigner transform at $\mathbf{r} = 0$ and $\mathbf{q} = 0$ are also given. The eigenvalue E_B is obtained by solving the S -wave Schrödinger equation Eq. (3.4) for $U_{\text{eff}}(R)$. The heading E_B (exact) indicates the exact eigenvalue, calculated from the $\Lambda\alpha$ Born kernel. The quark-model G -matrix interactions are fss2 and FSS both in the QTQ (qtq) and continuous (cont) prescriptions for intermediate spectra. The depth of the LS potential $U_{\text{eff}}^{LS}(0)$ is calculated from the q^2 value determined by using only the central force.

model	$V_W^C(0,0)$ (MeV)	q^2 (fm $^{-2}$)	$U_{\text{eff}}(0)$ (MeV)	$U_{\text{eff}}^{LS}(0)$ (MeV)	E_B (MeV)	E_B (exact)
SB	-58.86	1.062	-27.15		-1.86	-3.12
NS	-71.00	1.269	-31.85		-1.74	-3.12
ND	-32.08	0.613	-16.98		-2.38	-3.12
NF	-61.91	0.959	-24.83		-1.78	-3.12
JA	-74.35	1.168	-29.56		-1.60	-3.12
JB	-83.71	1.312	-32.81		-1.43	-3.12
fss2 (cont)	-29.53	0.731	-19.66	-17.22	-2.94	-3.62
fss2 (qtq)	-28.04	0.657	-17.99	-16.24	-2.15	-2.75
FSS (cont)	-26.35	0.673	-18.34	-11.50	-2.62	-3.18
FSS (qtq)	-25.95	0.607	-16.87	-12.30	-1.78	-2.29

while the others are short. This poor result of the RGM-WKB approximation for the $\Lambda\alpha$ interaction is probably related to the very strong nonlocality (or momentum dependence) originating from the P_r term in Eq. (3.1). In order to see this, we artificially changed the Majorana exchange mixture parameter u in Eq. (3.1) and compared E_B obtained by the Wigner transform technique and by the exact method using the $\Lambda\alpha$ Born kernel. Table 4 shows this comparison. The case $u = 2$ corresponds to pure Wigner-type $\Lambda\alpha$ interaction, which gives a local $\Lambda\alpha$ potential and complete agreement between the two methods. Once we decrease the u value and introduce the Majorana component, the Wigner transform technique loses the attractive effect of nonlocality very much and eventually reaches at a very weak effective local potential with no bound state before $u = 0$ (the strength of the odd force = -(the strength of the even force)). Our case is just in the middle of these two extremes, which corresponds to the approximate Serber-type interaction with a weak odd force. On the other hand, the exact solution is almost independent of the u value, which implies that the Λ -particle is bound to the α -cluster in the almost S wave.

The situation is almost the same even with the Wigner transform approach of the quark-model G -matrix interaction. We show in Fig. 4 solutions of the tran-

Table 4

Comparison of the S -wave bound-state energies calculated from the Wigner transform technique (E_B) and the Lippmann-Schwinger approach of the $\Lambda\alpha$ Born kernel ($E_B(\text{exact})$), when the Majorana exchange parameter u in Eq. (3.1) is changed from $u = 2$ (pure Wigner) to $u = 0$ (pure Majorana).

u	E_B (MeV)	E_B (exact) (MeV)
2	-3.219	-3.219
1	-1.864	-3.120
0.5	-1.272	-3.079
0	unbound	-3.041

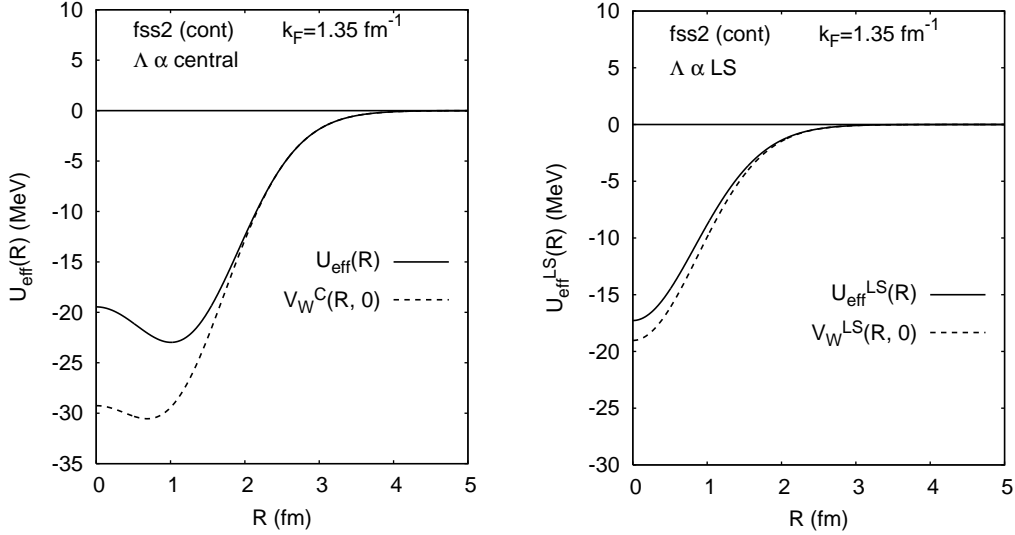


Fig. 5. The central component of Fig. 6. The same as Fig. 5, but for the the zero-momentum Wigner transform, LS component. The local momentum q is determined self-consistently by using the transcendental equation, $U_{\text{eff}}(R)$, for the quark-model G -matrix interaction fss2. The continuous choice for intermediate spectra is used for the G -matrix calculation.

scendental equations obtained from the Wigner transform of $\Lambda\alpha$ Born kernels. Here we also assumed $E = -3.12$ MeV. We find that different prescriptions for the G -matrix calculations, the QTQ (qtq) or the continuous (cont) choice for intermediate spectra, give essentially same result with a slightly smaller attraction for the QTQ . The model FSS gives a little weaker attraction than fss2. The bound-state energies listed in Table 3 show that the Schrödinger equation of $U_{\text{eff}}(R)$ gives smaller energies by $0.5 \sim 0.7$ MeV than the exact method using the $\Lambda\alpha$ Born kernel. In fact, the bound-state energy for ${}^5_{\Lambda}\text{He}$,

obtained by solving the Lippmann-Schwinger equation is -3.62 MeV for fss2 (cont) and -3.18 MeV for FSS (cont). These values are by no means too large, compared with the experimental value $E_B^{\text{exp}}({}^5_\Lambda\text{He}) = -3.12 \pm 0.02$ MeV. Table 3 also shows that the attraction is reduced when the the zero-momentum Wigner transform is converted to the effective local potential. This is depicted in Fig. 5 for a typical example of the fss2 prediction with the continuous prescription. The small difference of $V_W^C(0,0)$ values in Table 3 from those in Table 1 is because $r = 0.1$ fm and $q = 0.013$ fm $^{-1}$ is actually used in Table 1, instead of $r = q = 0$, and also because a spline interpolation for q is applied to $\mathcal{V}_0^C(k, q)$ in Eq. (2.35), to facilitate the Wigner transform for an arbitrary q . The LS component $U_{\text{eff}}^{LS}(R)$ depicted in Figs. 6 and 7, and the depth $U_{\text{eff}}^{LS}(0)$ in Table 3 are calculated from the LS Wigner transform in Eq. (2.35) by using local momentum q determined self-consistently for each R , with respect to the central component. First we find in Fig. 6 that the modification of the zero-momentum LS Wigner transform to the effective local potential is comparatively small. Secondly, Fig. 7 shows that the model FSS gives a shallower LS potential than model fss2, which is a result of the strong cancellation between the ordinary LS and the antisymmetric LS ($LS^{(-)}$) forces in the model FSS. In Fig. 8, we compare the central components of the effective local potentials obtained by the quark-model G -matrix interaction and by some of the effective ΛN forces. We find that the G -matrix prediction is rather long-ranged and situated in the middle of ND and SB predictions. It is convenient to parametrize the obtained $\Lambda\alpha$ potentials in simple Gaussian functions. For example, the effective local

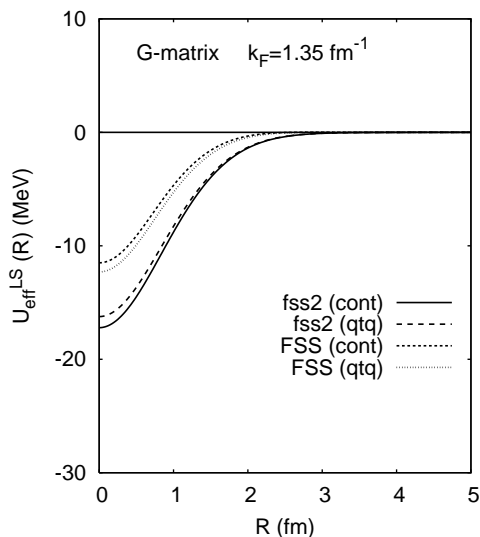


Fig. 7. The same as Fig. 4 but for the LS components. The local momentum is determined only by the central force.

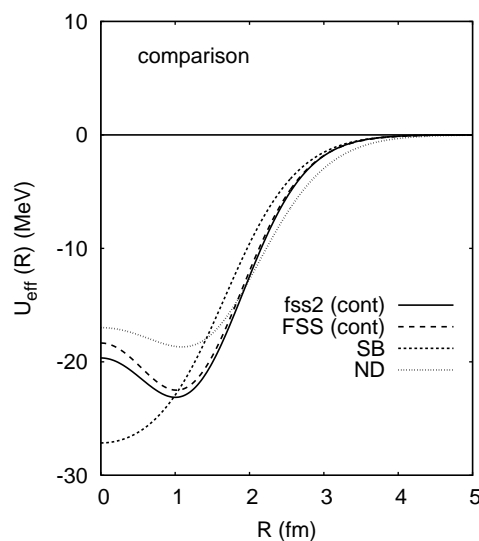


Fig. 8. Comparison of effective local potentials predicted by the quark-model G -matrix interactions fss2 and FSS with the continuous choice for intermediate spectra and by some of the effective ΛN forces, SB and ND potentials.

potential at $E = -3.12$ MeV, predicted by fss2 (cont) in Fig. 8, is expressed as

$$U(R) = -(19.42 + 19.50 R^2) e^{-0.5145 R^2} \quad (\text{MeV}) \quad , \quad (3.5)$$

with the bound-state energy $E_B = -2.95$ MeV (which corresponds to -2.94 MeV in Table 3).

We list in Table 5 the depths of the effective local potentials $U(0)$ for positive energies, $E_{\text{c.m.}} = 10, 30$ and 50 MeV, and the S -wave phase shifts $\delta_0^W(E)$ obtained by solving the Schrödinger equation. The exact phase shift $\delta_0(E)$

Table 5

The depths of the effective local potentials, $U_{\text{eff}}(0)$, and the S -wave phase shifts, $\delta_0^W(E)$, obtained by solving the Schrödinger equation. The exact phase shift, $\delta_0(E)$ (exact), is also shown, which is obtained by solving the Lippmann-Schwinger equation from the Born kernel.

model	$E_{\text{c.m.}}$ (MeV)	$U_{\text{eff}}(0)$ (MeV)	$\delta_0^W(E)$ (deg)	$\delta_0(E)$ (exact) (deg)
SB	10	-20.74	62.74	72.20
	30	-11.90	29.00	36.28
	50	-4.26	15.37	20.69
NS	10	-25.16	61.66	72.88
	30	-15.58	28.12	37.10
	50	-6.74	13.45	20.46
ND	10	-10.69	62.14	68.39
	30	-1.78	26.89	32.90
	50	6.29	12.83	17.94
fss2 (cont)	10	-15.33	70.58	74.82
	30	-9.46	36.24	40.54
	50	-4.04	22.47	25.75
fss2 (qtq)	10	-13.18	64.92	70.07
	30	-6.63	31.28	35.50
	50	-1.09	18.18	21.54
FSS (cont)	10	-14.90	69.70	73.49
	30	-9.79	36.88	40.50
	50	-4.96	23.01	26.62
FSS (qtq)	10	-12.21	62.64	67.88
	30	-6.10	30.25	34.30
	50	-1.27	18.14	21.20

(exact) is also shown, which is obtained from the Born kernel. Here we again find the effective local potentials are too shallow, especially for the effective ΛN forces. The phase shift difference is about $5 - 11^\circ$ for the effective ΛN forces, while $3 - 5^\circ$ for the quark-model G -matrix interactions. This implies that we need a readjustment of the effective local potentials of the order of 10 MeV, in order to reproduce the correct magnitude of the phase shifts.

3.2 $\Sigma\alpha$ and $\Xi\alpha$ interactions

As seen from Fig. 1, the $\Sigma\alpha$ and $\Xi\alpha$ interactions are repulsive. This does not mean that the Σ and Ξ potentials are always repulsive. The structure of spin-isospin factors for the $\Sigma\alpha$ and $\Xi\alpha$ systems is especially simple (see Eq. (2.10)), which is due to the spin-isospin saturated character of the α -particle. It is, therefore, important to examine each isospin component separately, in order to gain some insight to other possibilities of unknown hypernuclei. Here we discuss some qualitative features of these interactions, based on the symmetry

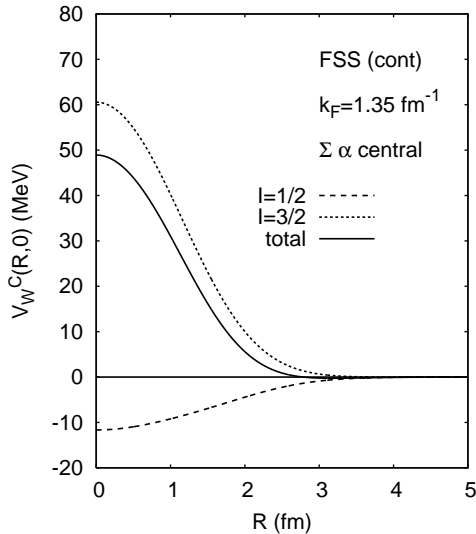


Fig. 9. The central components of the zero-momentum Wigner transform, $V_W^C(\mathbf{r}, 0)$ with $R = |\mathbf{r}|$, for the $\Sigma\alpha$ Born kernel, calculated from the quark-model G -matrix $B_8 B_8$ interactions by FSS. The Fermi momentum used in the G -matrix calculation is $k_F = 1.35 \text{ fm}^{-1}$ and the continuous choice is used for intermediate spectra. The $(0s)^4$ shell-model wave function with the h.o. size parameter $\nu = 0.257 \text{ fm}^{-2}$ is used for the α -cluster folding.

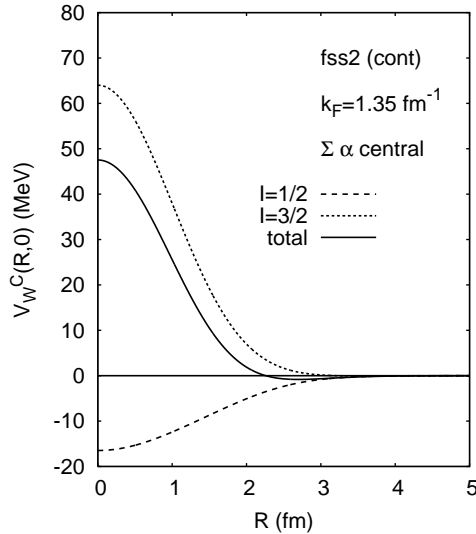


Fig. 10. The same as Fig. 9, but for fss2.

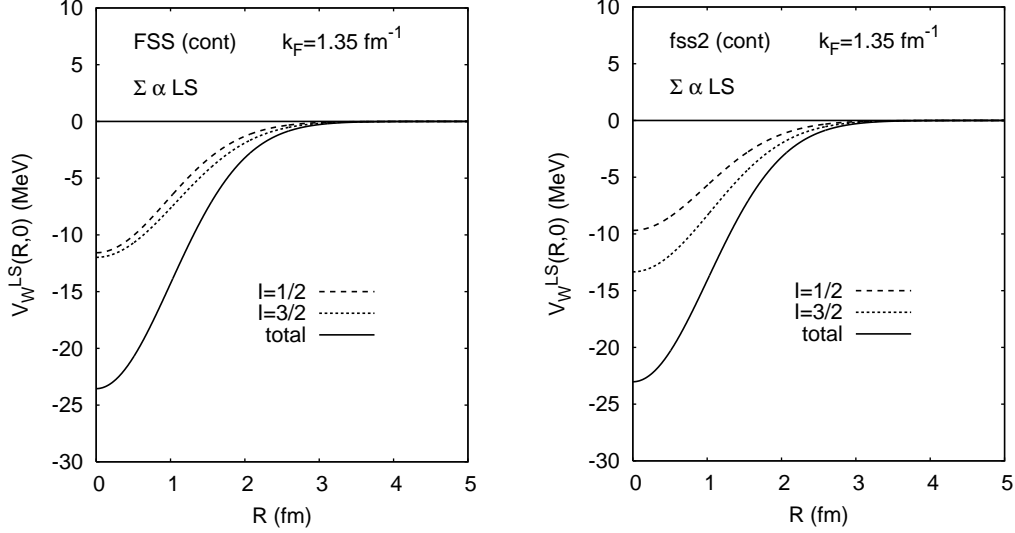


Fig. 11. The same as Fig. 9, but for the $\Sigma\alpha$ LS components. Fig. 12. The same as Fig. 11, but for fss2. LS components.

properties of the B_8B_8 interactions predicted by the quark-model interactions, FSS and fss2. When the interaction is repulsive, the transcendental equation Eq. (3.3) sometimes does not have its solution, since the square of the local momentum, q^2 , becomes negative. Since the extension of the Wigner transform Eq. (2.35) to the negative q^2 is not easy numerically, we only discuss the zero-momentum Wigner transform in this subsection.

Figures 9 and 10 show the isospin components with $I = 1/2$ and $I = 3/2$ for the $\Sigma\alpha$ central interaction, predicted by FSS and fss2, respectively. We find that both interactions have some amount of attraction originating from the 3S_1 channel of the $I = 1/2$ ΣN interaction. This channel becomes attractive due to the very strong ΛN - ΣN coupling by the one-pion exchange tensor force. On the other hand, the 3S_1 state of the $I = 3/2$ channel is strongly repulsive due to the Pauli principle at the quark level. We find from Figs. 9 and 10 that this repulsion is so strong that almost no attraction from the $I = 1/2$ channel remains in the $\Sigma\alpha$ interaction.

On the other hand, the two isospin channels, $I = 1/2$ and $3/2$, yield fairly large LS force for the $\Sigma\alpha$ interaction. This can be seen in Figs. 11 and 12. In the isospin $I = 3/2$ channel, 3P_J states are classified to the flavor symmetric channel with the SU_3 label (22). It is, therefore, plausible that the same mechanism as the NN $I = 1$ channel yields very strong LS force. On the other hand, a part of the LS force from the isospin $I = 1/2$ channel is due to the flavor-exchange process between $(11)_a$ and $(11)_s$ SU_3 configurations. This process is accompanied with the spin flip between $S = 0$ and 1, and yields very strong $LS^{(-)}$ force. The LS and $LS^{(-)}$ forces reinforce each other in just opposite way to the ΛN interaction, and the resultant $\Sigma\alpha$ LS force becomes

almost $3/5$ of the $N\alpha$ LS force, as seen from \tilde{S}_B in Table 1. This ratio is almost the same as that of the Scheerbaum factors $S_B = S_B(0)$ in symmetric nuclear matter. (See Table 2.)

Figures 13 and 14 show the isospin components with $I = 0$ and $I = 1$ for the $\Xi\alpha$ central interaction, predicted by FSS and fss2, respectively. Here again we find the situation that the attractive nature of the $I = 0$ component is largely canceled by the repulsion in the $I = 1$ channel. However, this cancellation is not strong especially in the model FSS, and we have almost 5 MeV attraction

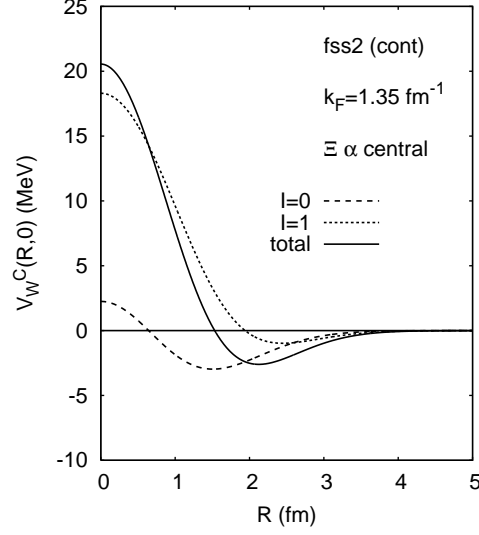
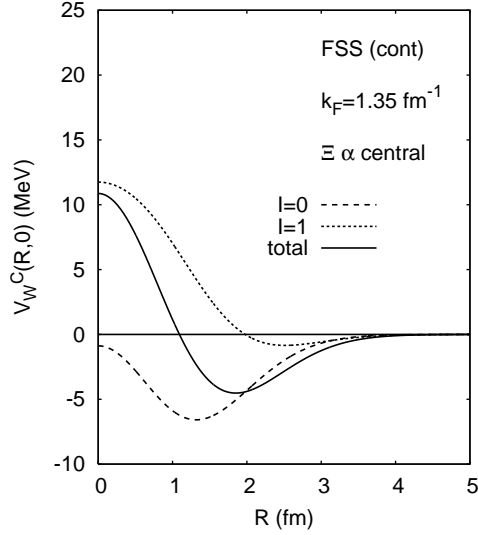


Fig. 13. The same as Fig. 9, but for the $\Xi\alpha$ interaction. Fig. 14. The same as Fig. 13, but for fss2.

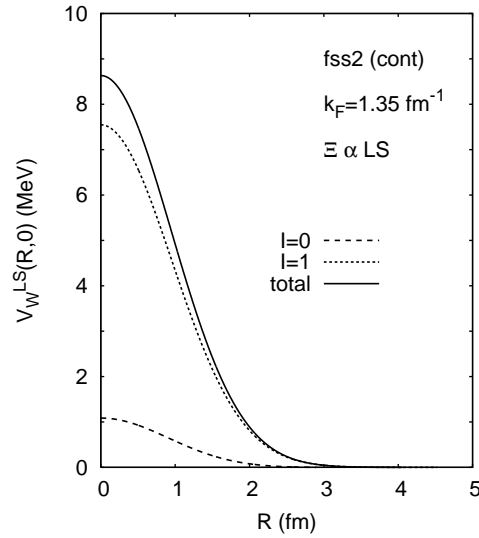
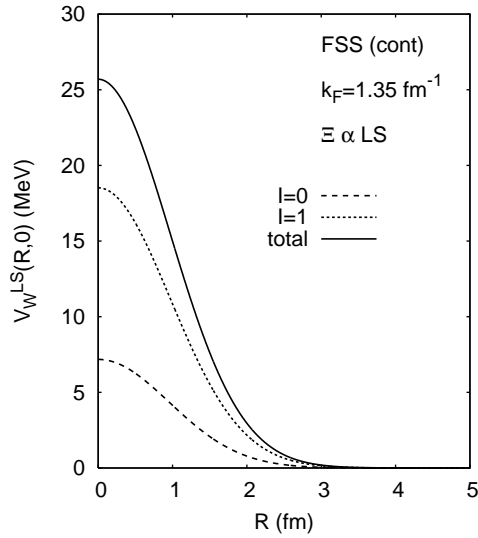


Fig. 15. The same as Fig. 13, but for the LS components. Fig. 16. The same as Fig. 15, but for fss2.

around $R = 2$ fm. In fss2, the height of the central repulsion in the $I = 1$ channel is almost 20 MeV, and we can expect a few MeV attraction in the surface region. These long-range attractions may have some influence to the atomic orbit between Ξ^- and α . It should be noted that the origin of the repulsion in the $I = 1$ channel is the Pauli forbidden state $(11)_s$ in the 1S_0 state and the almost Pauli forbidden state (30) in the 3S_1 state. However, the coupling with the $\Lambda\Sigma$ channel is very important, which may cause the long-range attraction even in the $I = 1$ channel.

The LS components of the $\Xi\alpha$ interaction is repulsive, which is clearly seen in Figs.15 and 16. This LS force is fairly strong, especially for FSS. The magnitude is almost 1/3 of the $N\alpha$ LS force with the opposite sign. These features are very similar to the LS force in symmetric nuclear matter, as seen in Table 2.

4 Summary

The SU_6 quark-model baryon-baryon interaction (fss2, FSS) [1,2,3] is a unified model which describes all the baryon-octet baryon-octet (B_8B_8) interactions in a full coupled-channel formalism. For the nucleon-nucleon (NN) and hyperon-nucleon (YN) interactions, all the available experimental data are reasonably reproduced. It is, therefore, interesting to study $B_8\alpha$ interactions in a microscopic framework under a simple assumption of the $(0s)^4$ harmonic-oscillator shell-model wave function for the α -cluster. In this study, we have used the result of G -matrix calculations for symmetric nuclear matter, as an input for the two-body interactions for the α -cluster folding. Since the resultant $B_8\alpha$ interactions are rather insensitive to the Fermi-momentum k_F in the G -matrix calculations (except for the ΛN LS force for FSS), we have assumed $k_F = 1.35$ fm $^{-1}$. The other G -matrix parameters, the center-of-mass (c.m.) momentum K of two interacting particles and the starting energy ω , are treated unambiguously in the total c.m. frame of the $B_8\alpha$ system. This can be achieved by considering the transformation of the matrix elements in the momentum representation from the initial (\mathbf{q}_i) and final (\mathbf{q}_f) momenta to the momentum transfer ($\mathbf{k} = \mathbf{q}_f - \mathbf{q}_i$) and the local momentum $\mathbf{q} = (\mathbf{q}_f + \mathbf{q}_i)/2$. If one uses this transformation at the level of G -matrix, the procedure of the α -cluster folding becomes extremely simple both for the central and LS components. The $B_8\alpha$ interaction, $\mathcal{V}^\Omega(\mathbf{k}, \mathbf{q})$ with $\Omega = C, LS$, represented by \mathbf{k} and \mathbf{q} is then transformed back to the $B_8\alpha$ Born kernel, $V^\Omega(\mathbf{q}_f, \mathbf{q}_i)$, through the inverse transformation. This procedure is also convenient to calculate the Wigner transform, $V_W^\Omega(\mathbf{r}, \mathbf{q})$, which is simply a Fourier transform of $\mathcal{V}^\Omega(\mathbf{k}, \mathbf{q})$. By solving the transcendental equation for $V_W^\Omega(\mathbf{r}, \mathbf{q})$, we can obtain an energy-dependent local potential of the $B_8\alpha$ system in the WKB-RGM approximation [22,23,20].

In this paper, we have applied the present formalism to the $\Lambda\alpha$, $\Sigma\alpha$ and $\Xi\alpha$ systems. Applications to the $N\alpha$ system will be discussed in a separate paper, since this system involves an extra nucleon-exchange term, in addition to the direct and knock-on terms. In the $\Lambda\alpha$ system, the WKB-RGM approximation is rather poor due to the very strong momentum dependence of the exchange knock-on term. This term appears even for the effective ΛN force, which is traced back to the strangeness exchange processes. We find that the $\Lambda\alpha$ central potentials predicted by various quark-model G -matrices are very similar to each other, irrespective of a specific model, fss2 or FSS, and the QTQ or continuous choice for intermediate spectra. At the bound-state energy, $E = -3.12$ MeV, they are long-range local potentials with the wine-bottle shape, having the depth less than 30 MeV. They are very similar to the $\Lambda\alpha$ potential obtained from the effective ΛN potential ND [18], simulating the Nijmegen hard-core model D. The $\Lambda\alpha$ bound-state energies are calculated by solving the Lippmann-Schwinger equation of the $\Lambda\alpha$ Born kernel. These are -3.62 MeV for fss2 (cont) and -3.18 MeV for FSS (cont). It should be noted that the depth of the single-particle potential for Λ in symmetric nuclear matter is 48 MeV for fss2 (cont) and 46 MeV for FSS (cont) [1]. The fact that the predicted $\Lambda\alpha$ bound-state energies are by no means too large, in comparison with the experimental value $E_B^{\text{exp}}({}^5_{\Lambda}\text{He}) = -3.12 \pm 0.02$ MeV, implies that the proper treatment of the c.m. motion of the $\Lambda\alpha$ system is very important. It is also important to note that, in the present G -matrix approach, the ΛN - ΣN coupling by the very strong one-pion exchange tensor force is explicitly treated, the lack of which is known to lead to the so-called overbinding problem of the $\Lambda\alpha$ bound state. The energy loss predicted by the α -cluster rearrangement effect [14] through the starting-energy dependence of the G -matrix needs further detailed analyses. On the other hand, the $\Lambda\alpha$ LS potentials are rather model dependent. In the model fss2, the depth of the LS potential is $-16 \sim -17$ MeV, while in FSS about -12 MeV. The interaction range of the FSS LS potential is also very short, which leads to a small Scheerbaum-like factor \tilde{S}_{Λ} for the $\Lambda\alpha$ LS force. We will show in a separate paper, the strength of the LS force is further reduced for smaller values of k_F , if FSS is used. The very small spin-orbit splitting of the ${}^9_{\Lambda}\text{Be}$ [24,25] can be reproduced in the $\alpha\alpha\Lambda$ Faddeev calculation, using the $\alpha\alpha$ RGM kernel and the $\Lambda\alpha$ LS Born kernel predicted from the FSS G -matrix with $k_F = 1.25$ fm $^{-1}$.

Based on the reasonable reproduction of the $\Lambda\alpha$ interaction properties, we have examined the real parts of the $\Sigma\alpha$ and $\Xi\alpha$ interactions in the Wigner transform technique. Since these interaction are repulsive, we have examined only the zero-momentum Wigner transform as the first step. In the $\Sigma\alpha$ interaction, the attractive effect from the isospin $I = 1/2$ ΣN channel is completely cancelled out by the repulsion from the $I = 3/2$ ΣN channel. The origin of this strong repulsion is the $\Sigma N(I = 3/2)$ 3S_1 channel, which contains the almost Pauli-forbidden SU_3 (30) component for the most compact $(0s)^6$ configuration. On the other hand, the $\Xi\alpha$ interaction is less repulsive because of the appreciable

attraction originating from the $I = 0$ ΞN channels. The $\Xi\alpha$ zero-momentum Wigner transform predicted by FSS yields about -5 MeV attraction around $R = 2$ fm, while the attraction of fss2 is about -3 MeV. These long-range attractions may have some relevance to the formation of atomic bound states for the $\Xi^-\alpha$ system. As to the spin-orbit interaction, the two isospin channels of the ΣN interaction give fairly strong attractive $\Sigma\alpha$ LS forces, yielding almost $3/5$ of the $N\alpha$ LS force. On the other hand, $\Xi\alpha$ LS force is repulsive and the magnitude is $1/8 \sim 1/2$ of the $N\alpha$ LS force. We will show in the next paper, the present $N\alpha$ LS force is consistent with the observed P -wave splitting of the $3/2^-$ and $1/2^-$ excited states of ${}^5\text{He}$.

It should be noted that the overall repulsive character of the $\Sigma\alpha$ and $\Xi\alpha$ interactions is related to the spin-isospin saturated character of the α -cluster. The strong isospin dependence of the ΣN and ΞN interactions, namely, repulsive for the $\Sigma N(I = 3/2)$ and $\Xi N(I = 1)$ channels and attractive for the $\Sigma N(I = 1/2)$ and $\Xi N(I = 0)$ channels, leads to a possibility of attractive features in some particular spin-isospin channels for systems of Σ , Ξ and the s -shell clusters. One of the examples of such systems is the isospin $I = 1/2$ and the spin $S = 0$ state of ${}^4_2\text{He}$, in which the strong repulsion of the $\Sigma N(I = 3/2)$ 3S_1 channel does not contribute [26] and a quasi-bound state is in fact observed experimentally [27]. Applications of the present approach to such systems are under way.

Acknowledgments

This work was supported by Grants-in-Aid for Scientific Research (C) from the Japan Society for the Promotion of Science (JSPS) (Grant Nos. 18540261 and 17540263).

A Invariant G -matrix for the most general B_8B_8 interaction

In this Appendix, we will define the invariant G -matrix for the most general B_8B_8 interaction. The B_8B_8 channels in the bra side (γ) and ket side (α) are specified by [20]

$$\begin{aligned}\gamma &= \left[\frac{1}{2}(11)c_1 \frac{1}{2}(11)c_2 \right] SS_z Y I I_z; \mathcal{P} \quad , \\ \alpha &= \left[\frac{1}{2}(11)a_1 \frac{1}{2}(11)a_2 \right] S' S'_z Y I I_z; \mathcal{P}' \quad ,\end{aligned}\tag{A.1}$$

in the isospin basis. For example, the spin-flavor functions are given by

$$\eta_\gamma = \chi_{SS_z} [B_1 B_2]_{II_z}^{\mathcal{P}} \quad ,$$

$$[B_1 B_2]_{II_z}^{\mathcal{P}} = \frac{1}{\sqrt{2(1 + \delta_{c_1, c_2})}} \left\{ [B_1 B_2]_{II_z} + \mathcal{P}(-1)^{I_1 + I_2 - I} [B_2 B_1]_{II_z} \right\} \quad , \quad (\text{A.2})$$

where the isospin-coupled flavor wave functions, $[B_1 B_2]_{II_z}$, are lexicographically ordered and the first baryon is numbered always 1 and the second 2 (i.e., $[B_2 B_1]_{II_z} = [B_2(1)B_1(2)]_{II_z}$). The flavor symmetry basis, $[B_1 B_2]_{II_z}^{\mathcal{P}}$ with $\mathcal{P} = 1$ and -1 , gives

$$[B_1 B_2]_{II_z} = \sqrt{\frac{1 + \delta_{c_1, c_2}}{2}} \sum_{\mathcal{P}} [B_1 B_2]_{II_z}^{\mathcal{P}} \quad ,$$

$$[B_3 B_4]_{II_z} = \sqrt{\frac{1 + \delta_{a_1, a_2}}{2}} \sum_{\mathcal{P}'} [B_3 B_4]_{II_z}^{\mathcal{P}'} \quad . \quad (\text{A.3})$$

The matrix element of the G -matrix in the isospin basis and its partial-wave decomposition are given by [21]

$$G_{\gamma\alpha}(\mathbf{p}, \mathbf{p}'; K, \omega) = \langle \chi_{SS_z} [B_1 B_2]_{II_z}^{\mathcal{P}} | G(\mathbf{p}, \mathbf{p}'; K, \omega) | \chi_{S'S'_z} [B_3 B_4]_{II_z}^{\mathcal{P}'} \rangle$$

$$= \sum'_{JM\ell\ell'} 4\pi G_{\gamma S\ell, \alpha S'S'_z}^J(p, p'; K, \omega) \sum_m \langle \ell m S S_z | JM \rangle Y_{\ell m}(\hat{\mathbf{p}})$$

$$\times \sum'_{m'} \langle \ell' m' S' S'_z | JM \rangle Y_{\ell' m'}^*(\hat{\mathbf{p}}') \quad . \quad (\text{A.4})$$

Here the prime symbol on \sum implies that the summation is only for such quantum numbers that satisfy the generalized Pauli principle:

$$(-1)^\ell (-1)^{1-S} \mathcal{P} = (-1)^{\ell'} (-1)^{1-S'} \mathcal{P}' = -1 \quad . \quad (\text{A.5})$$

We multiply Eq. (A.4) with $|\chi_{SS_z}\rangle$ and $\langle \chi_{S'S'_z}|$ from the left- and right-hand sides, respectively, and take a sum over SS_z and $S'S'_z$. Then we find

$$\langle [B_1 B_2]_{II_z}^{\mathcal{P}} | G(\mathbf{p}, \mathbf{p}'; K, \omega) | [B_3 B_4]_{II_z}^{\mathcal{P}'} \rangle$$

$$= \sum'_{JM\ell\ell'S S'} 4\pi G_{\gamma S\ell, \alpha S'S'_z}^J(p, p'; K, \omega) \mathcal{Y}_{(\ell S)JM}(\hat{\mathbf{p}}; \text{spin}) \mathcal{Y}_{(\ell' S')JM}^*(\hat{\mathbf{p}}'; \text{spin}) \quad ,$$

$$(\text{A.6})$$

where $\mathcal{Y}_{(\ell S)JM}(\hat{\mathbf{p}}; \text{spin}) = [Y_\ell(\hat{\mathbf{p}})\chi_S]_{JM}$ is the angular-spin function for the two-baryon system.

Let us denote the two-baryon channels with $c = (c_1, c_2)$, $a = (a_1, a_2)$, and consider

$$\begin{aligned}
& G_{ca}(\mathbf{p}, \mathbf{p}'; K, \omega) \\
& \equiv \langle [B_1 B_2]_{II_z} | G(\mathbf{p}, \mathbf{p}'; K, \omega) - G(\mathbf{p}, -\mathbf{p}'; K, \omega) P_\sigma P_F | [B_3 B_4]_{II_z} \rangle . \quad (\text{A.7})
\end{aligned}$$

We can rewrite this by using Eqs. (A.3) and (A.6):

$$\begin{aligned}
& G_{ca}(\mathbf{p}, \mathbf{p}'; K, \omega) \\
& = \frac{1}{2} \sqrt{(1 + \delta_{c_1, c_2})(1 + \delta_{a_1, a_2})} \sum_{\mathcal{P}, \mathcal{P}'} \left\{ \langle [B_1 B_2]_{II_z}^{\mathcal{P}} | G(\mathbf{p}, \mathbf{p}'; K, \omega) | [B_3 B_4]_{II_z}^{\mathcal{P}'} \rangle \right. \\
& \quad \left. - \langle [B_1 B_2]_{II_z}^{\mathcal{P}} | G(\mathbf{p}, -\mathbf{p}'; K, \omega) P_\sigma P_F | [B_3 B_4]_{II_z}^{\mathcal{P}'} \rangle \right\} . \quad (\text{A.8})
\end{aligned}$$

Here the second term in the brackets gives the same contribution as the first term, due to the condition Eq. (A.5). Thus we find that Eq. (A.7) is actually invariant G -matrix, which allows the expressions

$$\begin{aligned}
& G_{ca}(\mathbf{p}, \mathbf{p}'; K, \omega) \\
& = \langle [B_1 B_2]_{II_z} | G(\mathbf{p}, \mathbf{p}'; K, \omega) - G(\mathbf{p}, -\mathbf{p}'; K, \omega) P_\sigma P_F | [B_3 B_4]_{II_z} \rangle \\
& = \sqrt{(1 + \delta_{c_1, c_2})(1 + \delta_{a_1, a_2})} \sum_{\mathcal{P}, \mathcal{P}'} \langle [B_1 B_2]_{II_z}^{\mathcal{P}} | G(\mathbf{p}, \mathbf{p}'; K, \omega) | [B_3 B_4]_{II_z}^{\mathcal{P}'} \rangle \\
& = \sqrt{(1 + \delta_{c_1, c_2})(1 + \delta_{a_1, a_2})} \sum_{JM\ell\ell'SS'\mathcal{P}\mathcal{P}'} 4\pi G_{\gamma S\ell, \alpha S'S_z'}^J(\mathbf{p}, \mathbf{p}'; K, \omega) \\
& \quad \times \mathcal{Y}_{(\ell S)JM}(\hat{\mathbf{p}}; \text{spin}) \mathcal{Y}_{(\ell' S')JM}^*(\hat{\mathbf{p}}'; \text{spin}) \\
& = \sqrt{(1 + \delta_{c_1, c_2})(1 + \delta_{a_1, a_2})} [g_0 + g_{ss} (\boldsymbol{\sigma}_1 \cdot \boldsymbol{\sigma}_2) + h_0 i \hat{\mathbf{n}} \cdot (\boldsymbol{\sigma}_1 + \boldsymbol{\sigma}_2) \\
& \quad + h_- i \hat{\mathbf{n}} \cdot (\boldsymbol{\sigma}_1 - \boldsymbol{\sigma}_2) + \dots] . \quad (\text{A.9})
\end{aligned}$$

The eight independent invariant functions, g_0 , g_{ss} , etc., are expressed by some combinations of the partial-wave components of the G -matrix, $G_{\gamma S\ell, \alpha S'S_z'}^J(\mathbf{p}, \mathbf{p}'; K, \omega)$, which are explicitly given in Appendix D of Ref. [21].

References

- [1] Y. Fujiwara, Y. Suzuki and C. Nakamoto, to be published in Prog. Part. Nucl. Phys. (2006)
- [2] Y. Fujiwara, M. Kohno, C. Nakamoto and Y. Suzuki, *Phys. Rev. C* 64 (2001) 054001
- [3] Y. Fujiwara, T. Fujita, M. Kohno, C. Nakamoto and Y. Suzuki, *Phys. Rev. C* 65 (2002) 014002
- [4] Y. Fujiwara, K. Miyagawa, M. Kohno, Y. Suzuki and H. Nemura, *Phys. Rev. C* 66 (2002) 021001

- [5] Y. Fujiwara, K. Miyagawa, Y. Suzuki, M. Kohno and H. Nemura, *Nucl. Phys. A* 721 (2003) 983c
- [6] Y. Fujiwara, K. Miyagawa, M. Kohno and Y. Suzuki, *Phys. Rev. C* 70 (2004) 024001
- [7] Y. Fujiwara, K. Miyagawa, M. Kohno, Y. Suzuki, D. Baye and J.-M. Sparenberg, *Phys. Rev. C* 70 (2004) 024002
- [8] Y. Fujiwara, M. Kohno, K. Miyagawa and Y. Suzuki, *Phys. Rev. C* 70 (2004) 047002
- [9] Y. Fujiwara, M. Kohno, K. Miyagawa, Y. Suzuki and J.-M. Sparenberg, *Phys. Rev. C* 70 (2004) 037001
- [10] Y. Fujiwara, H. Nemura, Y. Suzuki, K. Miyagawa and M. Kohno, *Prog. Theor. Phys.* 107 (2002) 745
- [11] Y. Fujiwara, Y. Suzuki, K. Miyagawa, M. Kohno and H. Nemura, *Prog. Theor. Phys.* 107 (2002) 993
- [12] M. Kohno, Y. Fujiwara, T. Fujita, C. Nakamoto and Y. Suzuki, *Nucl. Phys. A* 674 (2000) 229
- [13] Y. Fujiwara, M. Kohno, T. Fujita, C. Nakamoto and Y. Suzuki, *Nucl. Phys. A* 674 (2000) 493
- [14] M. Kohno, Y. Fujiwara and Y. Akaishi, *Phys. Rev. C* 68 (2003) 034302
- [15] X. Campi and D. W. Sprung, *Nucl. Phys. A* 194 (1972) 401
- [16] M. Kohno, S. Nagata and N. Yamaguchi, *Prog. Theor. Phys. Suppl.* No. 65 (1975) 200
- [17] M. Kohno and D. W. L. Sprung, *Nucl. Phys. A* 397 (1983) 1
- [18] E. Hiyama, M. Kamimura, T. Motoba, T. Yamada and Y. Yamamoto, *Prog. Theor. Phys.* 97 (1997) 881
- [19] R. R. Scheerbaum, *Nucl. Phys. A* 257 (1976) 77
- [20] C. Nakamoto, Y. Suzuki and Y. Fujiwara, *Prog. Theor. Phys.* 94 (1995) 65
- [21] Y. Fujiwara, M. Kohno, C. Nakamoto and Y. Suzuki, *Prog. Theor. Phys.* 103 (2000) 755
- [22] H. Horiuchi, *Prog. Theor. Phys.* 64 (1980) 184 ; K. Aoki and H. Horiuchi, *Prog. Theor. Phys.* 68 (1982) 1658; 2028
- [23] Y. Suzuki and K. T. Hecht, *Nucl. Phys. A* 420 (1984) 525 ; 446 (1985) 749 (E)
- [24] H. Akikawa et al., *Phys. Rev. Lett.* 88 (2002) 082501
- [25] H. Tamura et al., *Nucl. Phys. A* 754 (2005) 58c
- [26] T. Yamada and K. Ikeda, *Prog. Theor. Phys.* 88 (1992) 139
- [27] T. Nagae et al., *Phys. Rev. Lett.* 80 (1998) 1605